ANALYTICAL AND EXPERIMENTAL STUDIES

ON

REINFORCED CONCRETE CLOSED FRAMES

by

Charles Wingfield Pryor, Jr.

Thesis submitted to the Graduate Faculty of the

Virginia Polytechnic Institute

in partial fulfillment for the degree of

MASTER OF SCIENCE

in

Structural Engineering

APPROVED:

Chairman, Dr. R. M. Barker

Dr. G. A. Gray

Dr. H. M. Morris

Prof. C. W. Smith

October, 1967

Blacksburg, Virginia

TABLE OF CONTENTS

		Page
ACKNOWLEDGMENTS		iii
LIST OF TABLES		iv
LIST OF FIGURES		v
Chapter		
I.	INTRODUCTION	1
II.	LITERATURE REVIEW	10
III.	THE INVESTIGATION	24
	A. Theoretical Analyses of Test Frames	24
	B. Experimental Program	36
	C. Test Results	48
IV.	DISCUSSION	60
V.	CONCLUSIONS	66
LITERATURE CITED		67
BIBLIOGRAPHY		69
VITA		72
APPENDIX A		73
APPENDIX B		84
APPENDIX C		88

ACKNOWLEDGMENTS

The author is indebted to for his suggestion of a research project which proved to be very interesting and enlightening. Appreciation is expressed to him for his guidance and constant assistance throughout the project.

Appreciation is due to of the Department of Agricultural Engineering for his providing the necessary test equipment, and to and his assistants for their help in the laboratory.

Acknowledgment is made to for his valuable suggestions and encouragement.

Appreciation is also expressed to the National Science Foundation, whose Trainee Program has financed the author throughout his graduate studies, and to the Civil Engineering Department for providing funds for the necessary materials for the experimental program.

Appreciation is expressed to for the typing of this thesis.

LIST OF TABLES

Table	Title	Page
1	Summary of Designs of Test Frames	35
2	Properties of the Test Frames	40
3	Comparison of the Predicted Ultimate Loads with the Actual Ultimate Loads	56
4	Load-Rotation Data for Frame No. 1 at the Center-line of Beam	74
5	Load-Rotation Data for Frame No. 1 at the Center-line of Column	75
6	Load-Rotation Data for Frame No. 2 at the Center-line of Beam	76
7	Load-Rotation Data for Frame No. 2 at the Center-line of Column	77
8	Load-Rotation Data for Frame No. 2 at the Left Support	78
9	Load-Rotation Data for Frame No. 2 at the Right Support	79
10	Load-Rotation Data for Frame No. 3 at the Center-line of Beam	80
11	Load-Rotation Data for Frame No. 3 at the Center-line of Column	81
12	Load-Rotation Data for Frame No. 3 at the Left Support	82
13	Load-Rotation Data for Frame No. 3 at the Right Support	83
14	Load-Deflection Data for Frame No. 1	85
15	Load-Deflection Data for Frame No. 2	86
16	Load-Deflection Data for Frame No. 3	87

LIST OF FIGURES

No.	Title	Page
1	Typical M-ϕ Relationship for Reinforced Concrete	3
2	Bilinear Approximation to the M-ϕ Curve	3
3	Elasto-Plastic Approximation to the M-ϕ Curve	5
4	Trilinear Approximation to the M-ϕ Curve	5
5	Example Problem	7
6	Multi-Linear Moment-Curvature Relationship	14
7	Bilinear Moment-Curvature Relationship	16
8a	Overall Dimensions of Frame	25
8b	Loading System	25
9	Elastic Moment Diagram - Frame No. 1	27
10	Final Design of Frame No. 1	27
11	Theoretical Moment-Curvature Curves for Frames No. 2 and No. 3	29
12	Moment and Curvature Diagrams - Bilinear	30
13	Final Design of Frame No. 2	33
14	Moment Diagram from Successive Moment Distribution	33
15	Stress-Strain Curves for the Reinforcing Steel	37
16	Statistical Stress-Strain Curves for the Concrete	39
17	Location of Strain Points on Frames	42
18	Straps and Clevices in Loading System	44
19	Load-Pressure Calibration Curve for Hydraulic Jacks	45
20	The Complete Test Setup	47
21	Possible Collapse Mechanisms for the Frames	49
22	Corner Failure Pattern of Frame No. 1	50

LIST OF FIGURES

No.	Title	Page
23	Total Collapse of Frame No. 1	50
24	Corner Failure Pattern of Frame No. 2	52
25	Steel Placement in Corner of Frame No. 2	52
26	Total Collapse of Frame No. 2	53
27	Premature Failure in the Corner of Frame No. 3	55
28	Comparison Between the Actual and the Theoretical Load-Rotation Curves	57
29	Comparison Between Load-Rotation Curves for Simple Beams with those of Frames	58
30	Load-Rotation Curves for Frames No. 2 and No. 3 at the Supports	59

I. INTRODUCTION

Desire has been expressed by a large number of researchers in the field of structural engineering to achieve a better understanding of the flexural behavior of reinforced concrete. More precisely, effort is being made to prove that reinforced concrete structural members can provide a desired amount of "ductility" under dynamic loads as well as static or gravitational loads.

Perhaps, the primary reason for dissatisfaction with current theory has been summed up by H. A. Sawyer[18] in his introductory remarks to the International Symposium on the Flexural Mechanics of Reinforced Concrete held in Miami, Florida in November of 1964. Sawyer cited that, "Present American design practice, as defined by ACI Building Code 318-63, specifies a non-elastic analytical determination of the ultimate strength of members at cross sections while specifying an elastic analytical determination of the moments and forces applied to the cross sections." This obvious inconsistency is the basis for the development of an inelastic, hence, a plastic analysis for reinforced concrete. However, since reinforced concrete is neither ideally elastic or plastic in behavior, a comprehensive method of analysis which relates prescribed failure-stages to their corresponding loads must be developed.

Currently, analytical methods, which relate failure-stages to loads through the moment-curvature (M-ϕ) relationship for reinforced concrete, are being presented. A characteristic of these methods is the provision that inelastic deformations (curvatures) are limited to

a predetermined value, which describes a certain least desirable failure-stage. This failure-stage may be narrow cracking, wide cracking, crushing and spalling, member collapse or total destruction. The question as to which failure-stage should be the limiting one needs a definite answer. This can be accomplished by accurate experimental verification of the proposed analytical methods.

A typical moment-curvature ($M - \phi$) relationship for a reinforced concrete cross section is shown in Figure 1. The previously described failure stages (narrow cracking, wide cracking, etc.) are defined by points on the curve. "Limit" analysis approximates the $M - \phi$ curve by straight lines intersecting at or near these failure points. Several recently proposed approximations are of particular interest to this writer, such as:

1. Bi-Linear Approximation - H. A. Sawyer [17] has proposed that the design of reinforced concrete frames be based on two failure stages and the $M - \phi$ relationship shown in Figure 2. The wide cracking failure stage is designed for by an elastic analysis according to line OA, the familiar elastic line, $\phi = M/EI$. The crushing-spalling failure stage is designed for by a bi-linear analysis according to lines OAB. The coordinates of point B are the ultimate curvature, ϕ_u, and the ultimate moment, M_u, as described by ACI 318-63. The point A is given by the elastic curvature, $\phi_e = M_e/EI$, and the moment M_e which is recommended as $0.85\ M_u$. The slope of the line AB depends on the plasticity factor, k_p, which

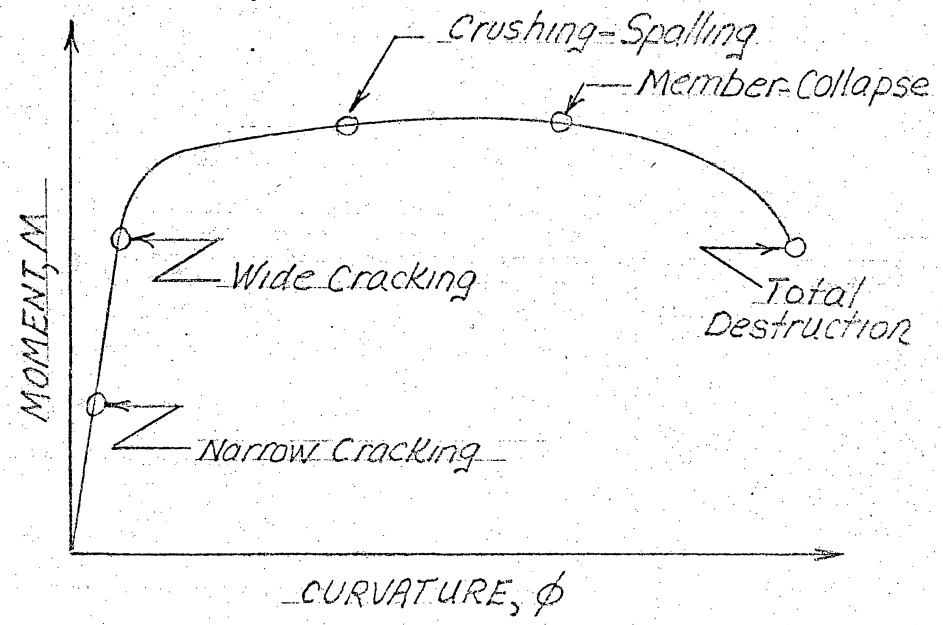

Figure 1. Typical M-ϕ Relationship for Reinforced Concrete

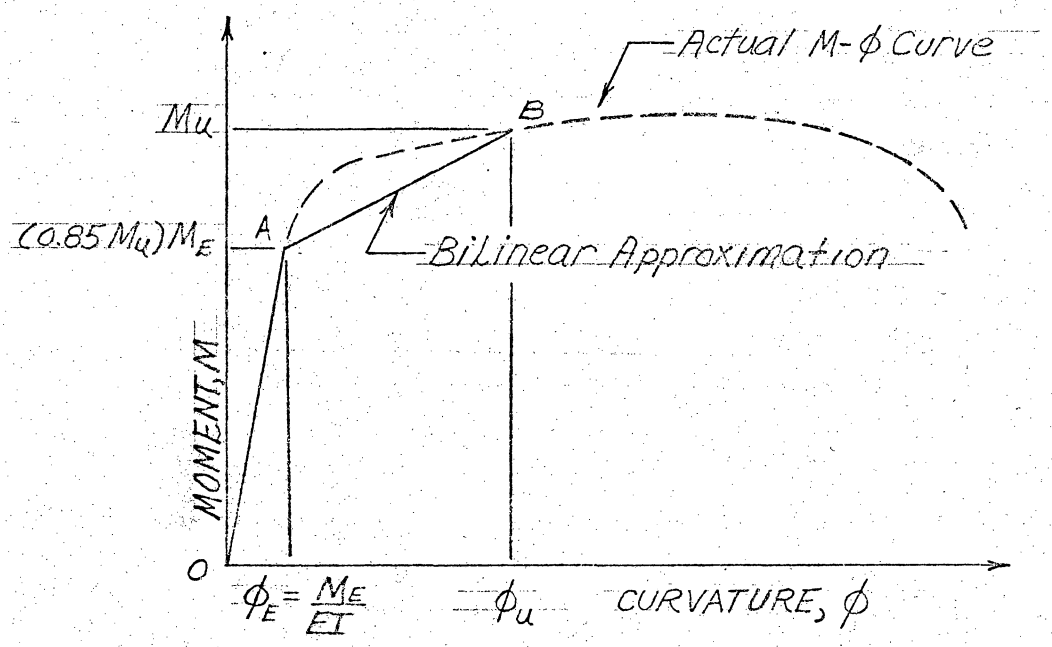

Figure 2. Bilinear Approximation to the M-ϕ Curve

is described in detail in Chapter II.

2. Perfect Elasto-Plastic Theory - The elasto-plastic approximation is similar to the bilinear approximation. The elastic line, which describes the wide cracking failure stage, extends from the origin to a yield moment, M_y, which is defined as 80% of the ultimate moment, M_u, provided by ACI 318-63. A perfectly plastic line extends from the point ϕ_y, M_y, at a constant moment, M_y, to a value of curvature at which a collapse mechanism for the structure is formed. See Figure 3.

Carl Berwanger[4] has proposed a successive moment distribution method of determining the location of the plastic hinges and the order in which they form. The first hinge forms at the point of maximum elastic moment when M_y is reached at that section, and then rotates at a constant moment, M_y, until the second hinge forms, and so on, until enough hinges are formed to produce a collapse mechanism for the structure.

3. Tri-Linear Approximation - Emilio Rosenblueth and Roger Díaz de Cossío [7] have proposed a tri-linear approximation to the $M - \phi$ curve shown in Figure 4. In addition to the lines OAB which describe the wide cracking and crushing-spalling failure stages, a third descending line, BC, defines the "strain softening" property of concrete. The phenomenon of a decreasing load accompanied by increasing deformations

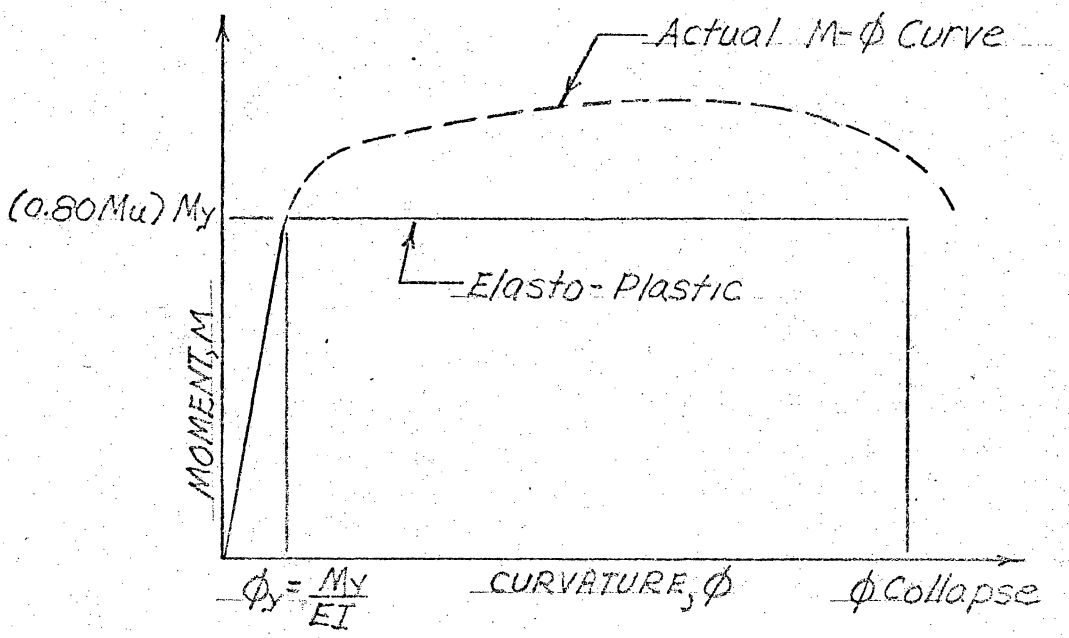

Figure 3. Elasto-Plastic Approximation to the M-ϕ Curve

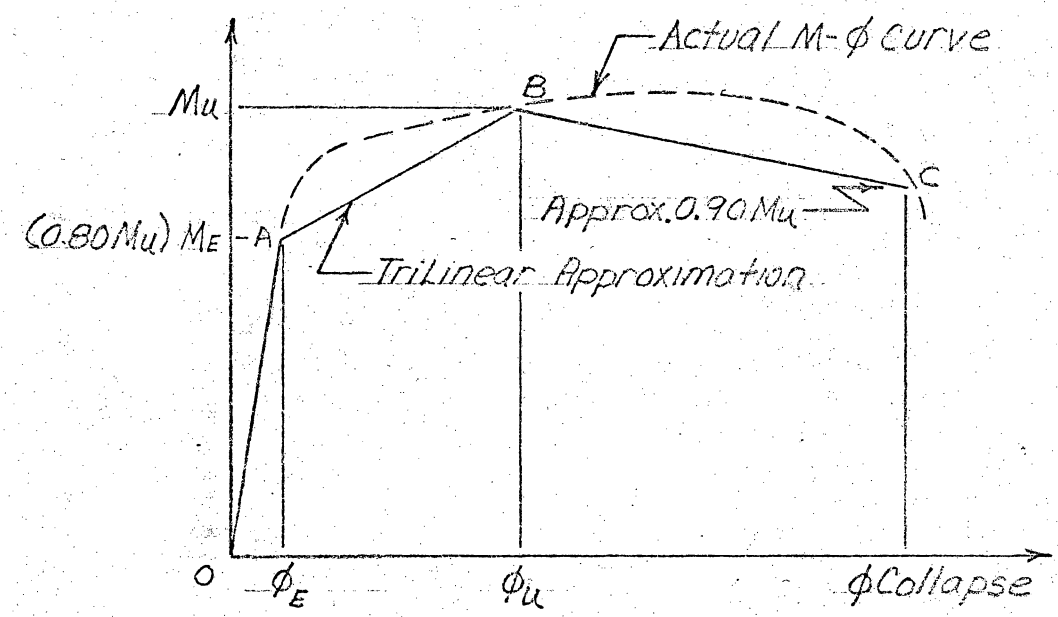

Figure 4. Trilinear Approximation to the M-ϕ Curve

is taken into account by the line, BC.

Both the Bi-linear and Tri-linear proposals provide for a spread of "contamination" which occurs at inelastic or hinging regions. A contamination length of d/2 to each side of the point of ultimate moment is assumed.

It should be noted that all of the above theories have one important dependency in common. The critical sections must be under reinforced to insure that failure is governed by yielding of the tension steel and not by crushing of the concrete. This is necessary for sufficient rotation to occur at the hinging regions to allow the moments to redistribute and form hinges in other sections, and eventually, a collapse mechanism for the structure. Over reinforced sections result in failure by concrete crushing, and do not allow the required rotational capacity for moment redistribution. Just how much rotational capacity or "ductility" reinforced concrete can offer is a vital question in the development of limit analysis.

One of the most important advantages which limit analysis offers the designer is a reduction of the congestion of reinforcement over the supports. As an example, a two span, continuous beam, shown in Figure 5, is designed for a concentrated ultimate load, P_u, of 25K at the mid-point of both spans.

An elastic analysis results in the design moments shown in the Elastic Moment Diagram of Figure 5. The design moment for the support Section B is 966 in-K.

Limit analysis allows for the design for any statically admissable

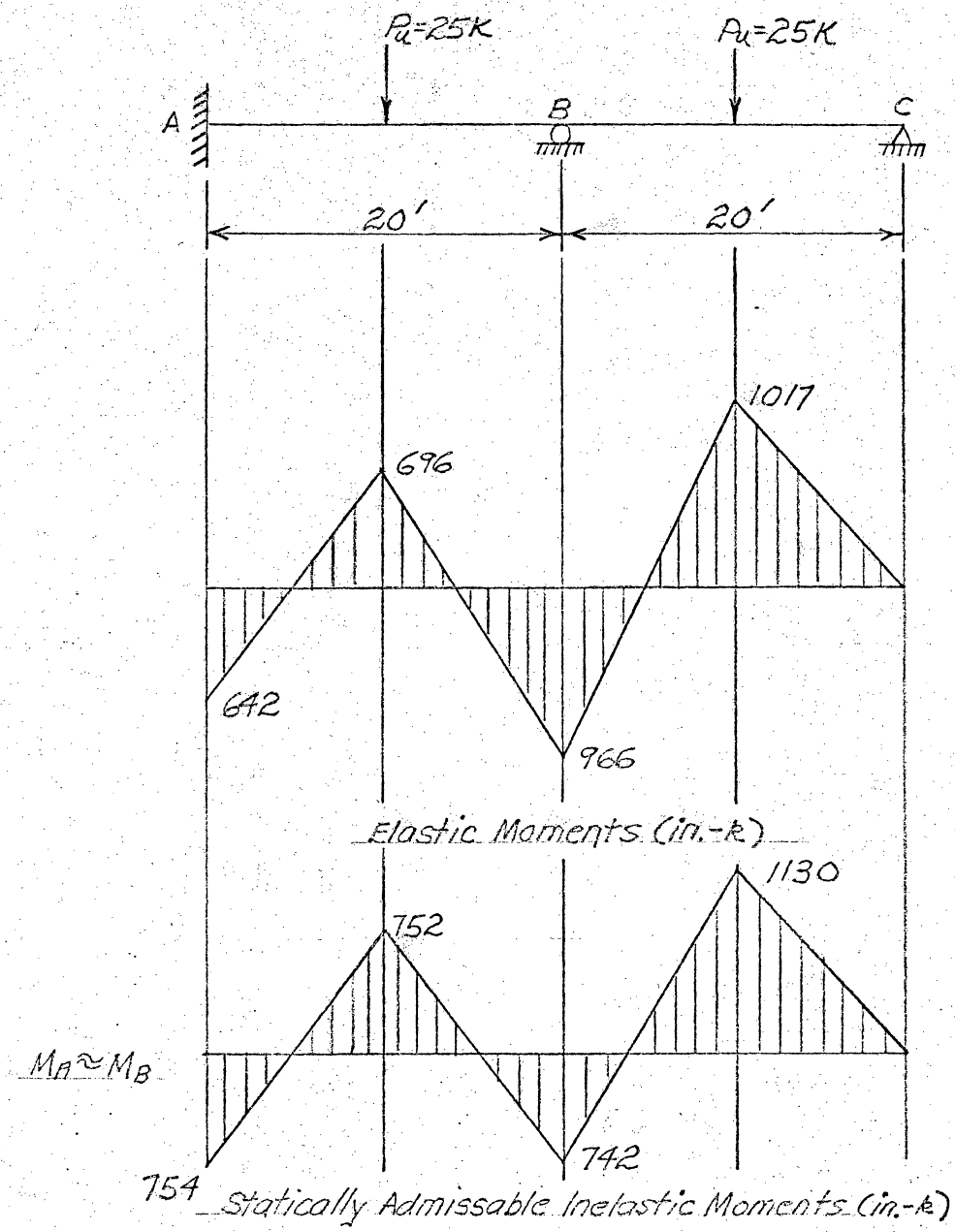

$$\text{Ratio,} \quad \frac{\text{Volume of Steel (Inelastic)}}{\text{Volume of Steel (Elastic)}} = 1.02$$

Figure 5. Example Problem

moment envelope. The Inelastic Moment Diagram shown in Figure 5 was selected because the moment at the fixed end, M_A, is approximately equal to the moment at support B, M_B. In this case, the design moment for the support section B is 742 in-K. Thus, for the same design load, limit analysis allows for a 23% reduction in reinforcement over the support. However, it should be noted that this is achieved at the expense of a 2% increase in total reinforcement.

Therefore, by being able to design for any statically admissable distribution of moments, the designer may either reduce reinforcement congestion or minimize the total amount of reinforcement, which ever is the most desirable. It does not appear that it is possible to achieve both in the same design; one is gained at the sacrifice of the other.

Like any other analytical procedure, limit analysis must be substantiated by laboratory test results. Unfortunately the tests must be more sophisticated since limit analysis correctly applies only to statically indeterminate structures; structures which display inelastic moment redistribution. In spite of the difficulties, tests must be carried out to provide valuable results helpful in understanding the behavior of reinforced concrete.

In this presentation, test results from the experimental studies on statically indeterminate reinforced concrete closed frames will be given. These results will be discussed and evaluated in the light of their contribution to a better understanding of the flexural behavior of reinforced concrete.

Three frames were built and analyzed; one by current practice, strictly adhering to ACI Building Code 318-63 and two by the previously discussed limit analysis. The bi-linear approximation with an assumed contamination length and the successive moment distribution method using the perfect elasto-plastic moment-curvature curve were the methods used to analyze the last two frames. These analytical results will be compared with the experimental test results in the hope of achieving a reasonable correlation.

The parameters investigated were the net reinforcing index $(q-q')$, the amount of transverse reinforcement, and the placement of steel in the beam-column joints. Factors of interest are the contribution of transverse reinforcement and compression steel to the rotational capacity of the hinging regions and the affects of steel placement and concrete cover on the load carrying capacity.

There was no definite way of experimentally determining the moments in the frames. Therefore, results will be expressed in the form of load-rotation curves instead of moment-rotation curves. The theoretical analyses and numerical calculations are shown in Chapter III, THE INVESTIGATION.

II. LITERATURE REVIEW

Professor A. L. L. Baker[1] made considerable progress in developing a plastic theory for reinforced concrete design as early as 1949. He derived a general expression for the ultimate strength in bending of ordinary reinforced concrete, taking into account plasticity. Also, a method of calculating elasto-plastic deformation was developed and applied to the problem of redistributing bending moments in continuous members and frames. His basic assumption for the ultimate strength of reinforced concrete beams in bending was:

> A beam is loaded to its ultimate strength when the concrete begins to crush either,
>
> 1. without the steel yielding,
> 2. on account of the steel yielding and causing the neutral axis to rise, or
> 3. the steel reaches a stress at which a small number of further repetitions of load would cause increased yield and fracture.

The final expression for the ultimate strength in bending was given as,

$$M = \alpha\, bd^2\, c\, (n_1 - \gamma n_1^2)$$

where n_1 was defined as,

$$n_1 = -p_s + \left(\sqrt{p_s^2 + 200\, p_s/zm \times zm/100} \right)$$

and,

M = ultimate bending moment

d = effective depth of beam

c = concrete stress at the extreme fiber

$n_1 d$ = depth to neutral axis

$\beta n_1 d$ = depth to center of concrete stress diagram

$\alpha n_1 dc$ = area of concrete stress diagram

p_s = steel percentage

z = a constant taken as unity for ordinary theory

$m = E_s/E_c$ the ratio of the modulus of plasticity of steel to that of concrete.

From his expression for the ultimate bending moment, Baker then derived the familiar expression for the curvature of a beam in bending,

$$\phi = M/EI$$

He concluded from his investigation the following:

1. Plasticity of concrete considerably increases the ultimate concrete moment of resistance, but does not greatly influence the redistribution of bending moments in continuous members, as the reduction in E_c is small.
2. Reinforcement yield can provide adequate moment redistribution, but may be limited by weakening of the steel or excessive rise of the neutral axis.

W. W. L. Chan [2], in conjunction with A. L. L. Baker, investigated the idealized plastic hinge assumption, which is that plastic hinges concentrated at points develop their full plastic moments of resistance, while framework members between hinge points remain elastic. This was said to be satisfactory if the required plastic deformations at the hinge points did not cause the ultimate strain capacity of the concrete

to be exceeded. If this happened, the degree of moment redistribution would be reduced unless the ultimate strain could be increased in some way. Thus, tests were conducted on short specimens of concrete, bound by lateral ties, pinned at both ends and subjected to compression loading of small eccentricity. The main variable was the ratio of lateral binding. From the test results, Chan concluded,

1. Spalling of concrete cover and hence reduction of concrete compression area caused an abrupt drop of load, but lateral binding enabled the enclosed concrete to continue to resist load.
2. Circular binding was distinctly more efficient than retangular binding in affording lateral support to the contained concrete.

In 1962, Chan [3] published a paper on "The Rotation of Reinforced Concrete Plastic Hinges at Ultimate Load." He observed that concrete brittleness makes it necessary to ensure that rotations required at plastic hinges do not exceed the rotation capacities for which a distribution of ultimate bending moments is admissable. The available rotation at a plastic hinge was given by the expression,

$$\theta_p = \int_0^{h_1 z} M \left(\frac{1}{EI_u} - \frac{1}{EI_e} \right) ds$$

in which,

$h_1 z$ = length of plastic hinge

M = moment at the section considered

EI_u = plastic value of EI

EI_e = elastic value of EI

From a study of 67 beam and column tests, Chan concluded that,

1. Local modifications to reinforcement can be made at plastic hinges to reduce the neutral axis depth.
2. Short lengths of compression steel can be introduced or modified locally to bring about significant increases in rotation capacity without, in most cases, disturbing the ultimate moment.
3. For even larger increases in rotation capacity, close-spaced binders can be added in the hinging regions.

The proceedings of the International Symposium on the Flexural Mechanics of Reinforced Concrete offered many excellent papers on current developments in reinforced concrete theory. Herbert A. Sawyer, Jr.[4] presented a very interesting keynote survey, in which he discussed a method of comprehensive analysis based on a multilinear moment-curvature relationship using critical moments and "plasticity factors." Referring to Figure 6, the plasticity factor, K_{2p}, was defined as the factor by which the "elastic-limit" curvature, ϕ_{1e}, must be multiplied to obtain the corresponding intercept, $K_{2p}\,\phi_{1e}$. From the similar triangles defined by base $K_{2p}\,\phi_{1e}$ and point (1) and base ϕ_{2p} and point (2), the value of curvature, ϕ_{2p}, was given as,

$$\phi_{2p} = \frac{\phi_{1e}}{M_{1e}} \; (K_{2p}) \; (M - M_{2e})$$

Adding all curvatures by such pairs of similar triangles, the total curvature for a moment in the segment immediately above point "n" was given as,

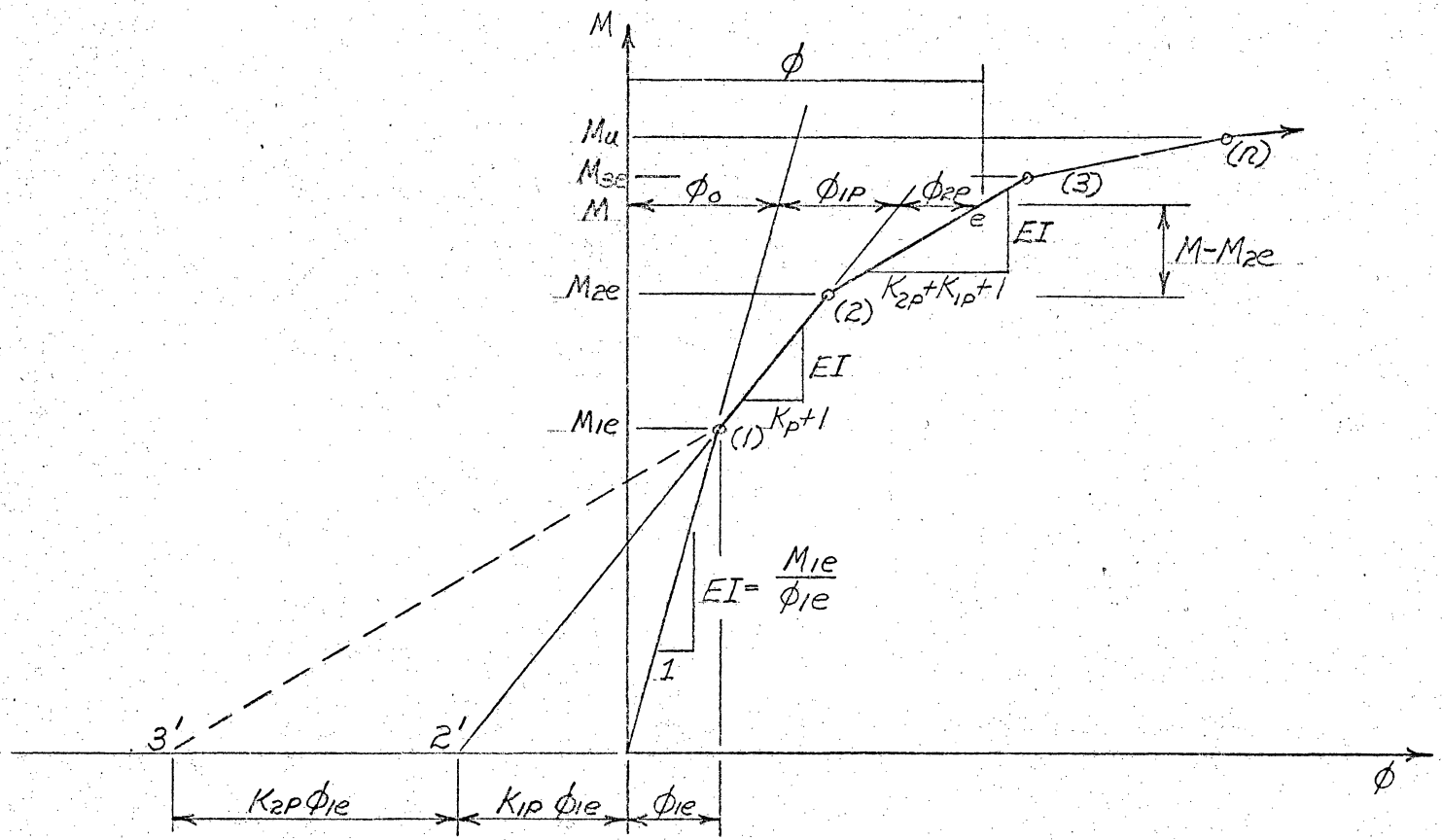

Figure 6. Multi-Linear Moment-Curvature Relationship

$$\phi = \frac{\phi_{1e}}{M_{1e}} \left[M + K_{1p}(M - M_{1e}) + K_{2p}(M - M_{2e}) + \ldots + K_{np}(M - M_{ne}) \right]$$

From this, Sawyer concluded,

1. For calculations of rotations and deflections from multi-linear curvatures, the same moment-area principles used for purely elastic curvatures may be used if, in addition to the total moment-area, the total area above M_{1e} expanded by the factor K_{1p}, the total area above M_{2e} expanded by the factor K_{2p}, and the total area above M_{ne} expanded by K_{np} are also included.
2. With this simple evaluation of curvatures in terms of moments, each stage in the comprehensive analysis of a structure consists of arriving at a statically admissable set of moments for which the curvatures, rotations and deflections satisfy the structure's boundary conditions.

In addition to his keynote survey paper, H. A. Sawyer (5) described a bilinear design procedure for concrete frames for two failure stages. The two failure stages were described as,

1. Wide cracking, in which an elastic analysis would be used for stresses at a section and for a distribution of moments.
2. Crushing-spalling, in which a conventional ultimate strength analysis would be used at sections, and an analysis based on a bilinear moment-curvature relationship and plasticity factors would be used for the distribution of moments.

The idealized bilinear moment-curvature curve is shown in Figure 7. An outline of the procedure for using bilinear analysis was given

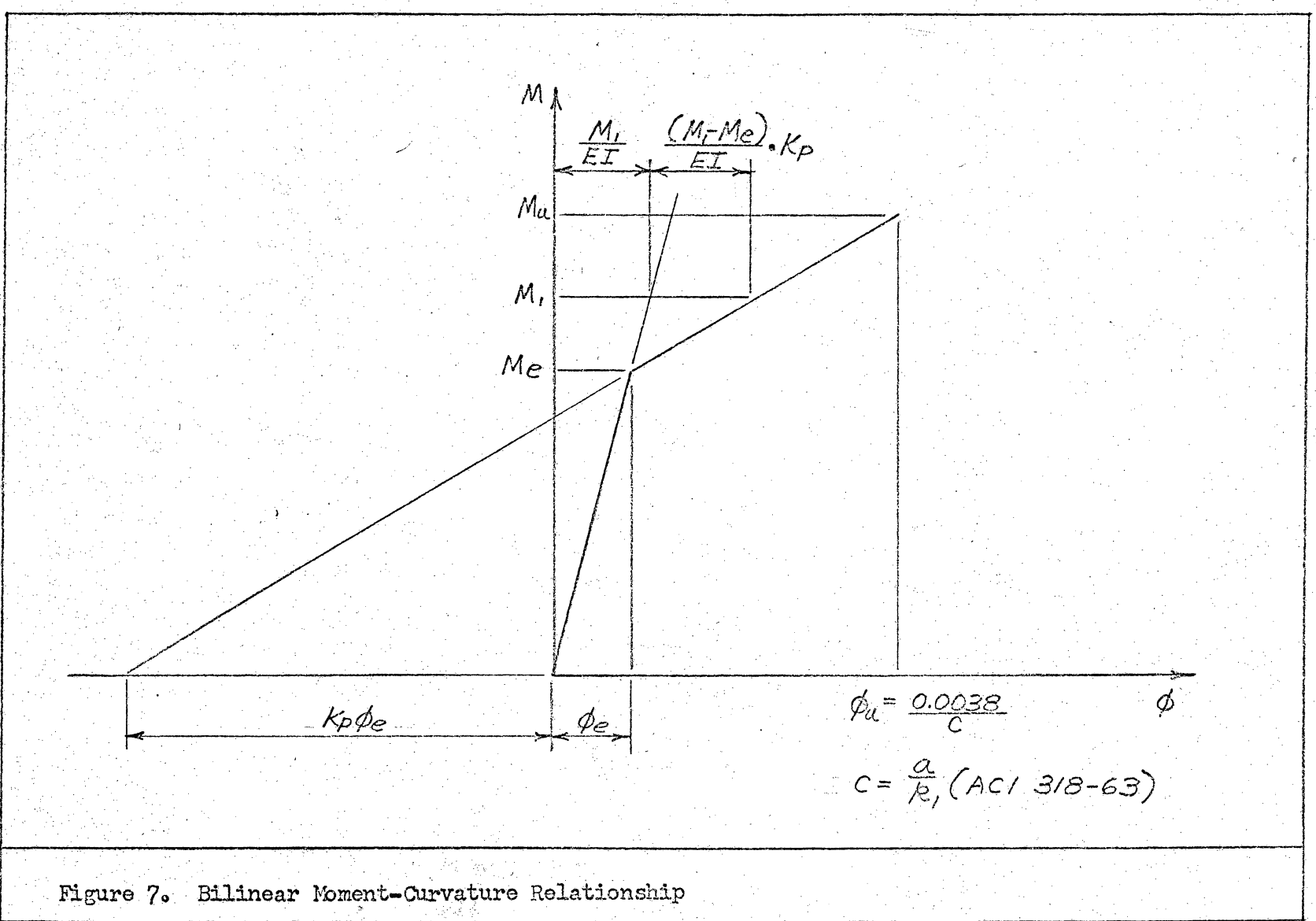

Figure 7. Bilinear Moment-Curvature Relationship

as follows:

1. Construct an M_u diagram corresponding to reinforcement. M_u is the ultimate moment defined by ACI 318-63. Sketch in values of M_e's which are recommended as 0.85 M_u's. (The 0.85 is considered better than the 1.00 used in elastic analysis)

2. For each possible critical combination of ultimate loading, using any set of adjusted moments which satisfy statics and falls within the M_u's provided, calculate the corresponding inelastic bending angles (K_p times inelastic moment-area) for each plastic region.

3. Calculate, elastically, the moments induced by these bending angles. If these moments nowhere exceed the M_u's of step No. 1, compute the ultimate loads for the crushing-spalling failure stage.

The plasticity factor, K_p, was given by the expression,

$$K_p = \frac{0.28\ E_s(1-K/3)\ (1-K)}{f_y[\ 1-1.38(q-q')\ ][\ 1-0.59(q-q')]} - 6.67$$

This equation applies to members with both tension and compression reinforcement. If $(q-q')$ is less than 0.06, it is recommended that $(q-q')$ be set equal to 0.06 in the equation for K_p. The notation for the equation was given as,

E_s = modulus of elasticity of steel

$(q-q')$ = net reinforcing index

f_y = yield stress of reinforcing steel

K = ratio of distance; outer compression fiber
to neutral axis at transformed cracked section to d

Graphs of K_p versus $(q-q')$ for different values of f_y were given in the paper.

For theoretical considerations, an extension of inelasticity at the hinging regions was recommended. The recommendation was that the inelastic length should be extended a distance, d/2, at each maximum moment concentration without otherwise changing the shape of the inelastic moment-area (i.e. a triangular area would remain triangular).

In comparison with other methods, some of the advantages of bilinear analysis were given as,

1. the minimizing of reinforcing steel
2. the reduction of congestion of reinforcement
3. an evaluation of the moments in the structure when M_u is first attained
4. any statically admissable moment envelope may be designed for, instead of being restricted to a 10% negative moment deviation from elastic moments.

An analysis of experimental test results showed an average ratio of test strength to calculated strength (using bilinear analysis) for under-reinforced continuous beams was 1.156.

In 1966, Carl Berwanger [6] presented a method of using successive moment distribution in limit analysis. The assumptions for the method were,

1. A perfect elasto-plastic structural behavior
2. None of the actual ultimate moment capacities are reached at

any of the critical sections due to a ductile ultimate loading system.

3. The rotational capacity, ϕ_{max}/ϕ_y, must be adequate enough at the early forming hinges to assure the formation of a collapse mechanism.

An outline of the procedure for using the successive moment distribution was given as:

1. Determine M_y (yield moment) by an initial plastic analysis for the proportioning of sections.
2. Establish relative Moments of Inertia of the critical sections from the corresponding M_y's.
3. Make successive elastic moment distributions to determine the order of formation and location of the first and subsequent hinges. Once M_y is reached at a section, the hinge is assumed to have zero additional moment capacity.
4. Calculate required rotation capacities by the conjugate beam method.

The necessary expressions were:

1. $$M_y = \frac{f_c K' b d^2 (1 - K'/3)}{2 + A_s f_s' K'' d}$$

(for sections with both tension and compression reinforcement)

Simplyfying the above expression for M_y,

2. $M_y = 0.80 M_u$

(M_u defined by ACI 318-63)

3. Rotational capacity, $\frac{\phi_{max}}{\phi_y} = \frac{0.0274\ EI}{bd^3q^2f_c'}$

Simplyfying by assuming $I = bd^3/12$ and $E = 1000f_c'$,

4. $\phi_{max}/\phi_y = 1/(4q^2)$

for which,

f_c = unit compressive stress in concrete

$K'd$ = depth to transformed area of steel

$K''d$ = distance between centers of tension and compression steel

A_s' = area of compression steel

E = modulus of elasticity of concrete

I = moment of inertia of the transformed cracked section

f_s' = stress in the compression steel

f_c' = concrete compressive strength

d = effective depth of steel

$q = p\ f_y/f_c'$ where $p = A_s/bd$

$q' = p'f_y'/f_c'$

Emilio Rosenblueth and Roger Díaz de Cossío (7) investigated the inadequacy of the nonlinear moment-curvature approach to treat systems which exhibit a descending branch in their generalized force-deformation relation. A procedure was presented, based on a moment-rotation approach and the assumption of a certain "contaminated" length of the beam near the regions of maximum moment which could take into account the descending branch and predict an increasing rotation or deflection with decreasing moment. The shape of the descending branch was said to

depend on the stiffness of the loading system.

The authors point out that crushing of concrete is a case of instability and should not be treated as a material failure. A spread of contamination of 1/2 to 1 effective depth to each side of the most highly stressed sections was said to be adequate under most conditions.

H. E. H. Roy and Mete A. Sozen [8] carried out tests on 60 axially loaded 5" by 5" by 25" prisms. The major variables for the experimental program were the spacing of transverse ties and the amount of longitudinal reinforcement. The volumetric ratio of the transverse reinforcement was kept constant at 0.02. The primary objective of the investigation was to obtain data on the load-deformation curve of concrete as related to the rotation capacity of reinforced concrete connections.

Test results indicated the following:

1. Square ties, with or without longitudinal reinforcement, did not enhance the load carrying capacities of the concrete in the specimen.
2. Ties considerably increase the deformation capacity or ductility of the concrete.

Vitelmo V. Bertero and C. Felippa [9] carried out a series of tests on beams subjected to pure bending moment in the center regions. From test results the authors concluded:

1. The addition of ties can improve the rotation capacity of reinforced concrete members in pure bending.

2. Proper combination of ties and compressive reinforcement may offer economic advantages and perhaps result in better overall behavior.

A series of compression tests carried out on specimens similar to those of Roy and Sozen[8], resulted in a different conclusion. Bertero and Felippa found that ties, with and without longitudinal reinforcement, did enhance the load-carrying capacity of the concrete in the prisms.

Alan H. Mattock[10] conducted an investigation on the rotational capacity of hinging regions in reinforced concrete beams. Tests were conducted on 37 beams involving the variables of concrete strength, depth of beam, distance from point of maximum moment to point of zero moment and amount and yield point of reinforcement. The specimens consisted of simple-span beams subjected to a concentrated load at midspan. The system simulated the distribution of bending moments adjacent to a support in a continuous beam. Mattock concluded the following from his investigation:

1. Maximum concrete compressive strain in a reinforced concrete beam at a section of maximum moment under a single concentrated load or over a support can be very much in excess of the usually assumed value of 0.003.
2. The spread of plasticity along the beam away from the section of maximum moment was found to increase with an increase in the ratio of z/d (z = the distance from the maximum moment to the point of contraflexure) and with a

decrease in the net tension reinforcement expressed as $(q-q'/q_b)$.

A safe limiting value for the maximum concrete strain under the conditions in the test program was given as,

$$\varepsilon_u = 0.003 + 0.5/z$$

(z is in inches)

The ratio of the total inelastic rotation, θ_{tu}, in the length z, to the inelastic rotation, θ_u, in length d/z, was expressed as,

$$\frac{\theta_{tu}}{\theta_u} = 1 + (1.14\sqrt{\frac{z}{d}} - 1)\left[1 - (\frac{q-q'}{q_b})\sqrt{d/16.2}\right]$$

E. O. Pfrang, C. P. Siess and M. A. Sozen[11] presented a method of relating load, moment and curvature for reinforced concrete members in combined bending and axial load. The method consisted of determining a sufficient number of discrete points relating P, M and ϕ to describe the load-moment-curvature relationship for the section. The procedure was given as follows:

1. Assume a linear strain distribution over the length of the section.
2. Assume stress-strain relationships for the concrete and reinforcement and determine the stress distribution over the cross section.
3. Sum algebraically the normal stresses over the area on which they act to determine the axial load, P.
4. Sum bending moments caused by the normal stresses to obtain the resultant bending moment, M.
5. Compute the angle between the line representing the strain distribution and the zero strain line to determine the curvature, ϕ.

III. THE INVESTIGATION

A. Theoretical Analyses of Test Frames

All three frames tested had the same overall dimensions (See Figure 8a). The distance between the centerlines of the columns was 6 feet and between the centerlines of the beams, 5 feet. Outside dimensions were 6' 7" in width by 5' 7" in height. For construction conveniences, the cross sectional dimensions for both the beams and the columns were made 4 inches in width and 7 inches in depth.

Three concentrated loads were to be applied at the quarter points of the beam members by hydraulic jacks, connected to the same pressure line, pulling in tension. The centerline dimensions were used as reference lines for the application of the loads (See Figure 8b). The system simulated the loading of a section of a box culvert, not considering the lateral earth pressures on the sides.

Frame No. 1 was designed by current practice, using the ultimate strength design provided by ACI Building Code 318-63. A conventional elastic analysis gives the moment diagram shown in Figure 9. The maximum moment, in terms of the load, P, and length, L, is seen to occur at the midspan of the beams and be equal to 0.330 PL.

The balanced steel percentage (p_b), assuming a yield stress for steel (f_y) of 40 ksi and a concrete compressive stress (f_c') of 3 ksi, is 0.0371. The maximum steel percentage (p_{max}) given by the code as 75% of the balance steel percentage, is 0.0278. Thus, if two No. 4 bars (A_s = 0.40 in.^{2}) were used in the midspans of the beams, the

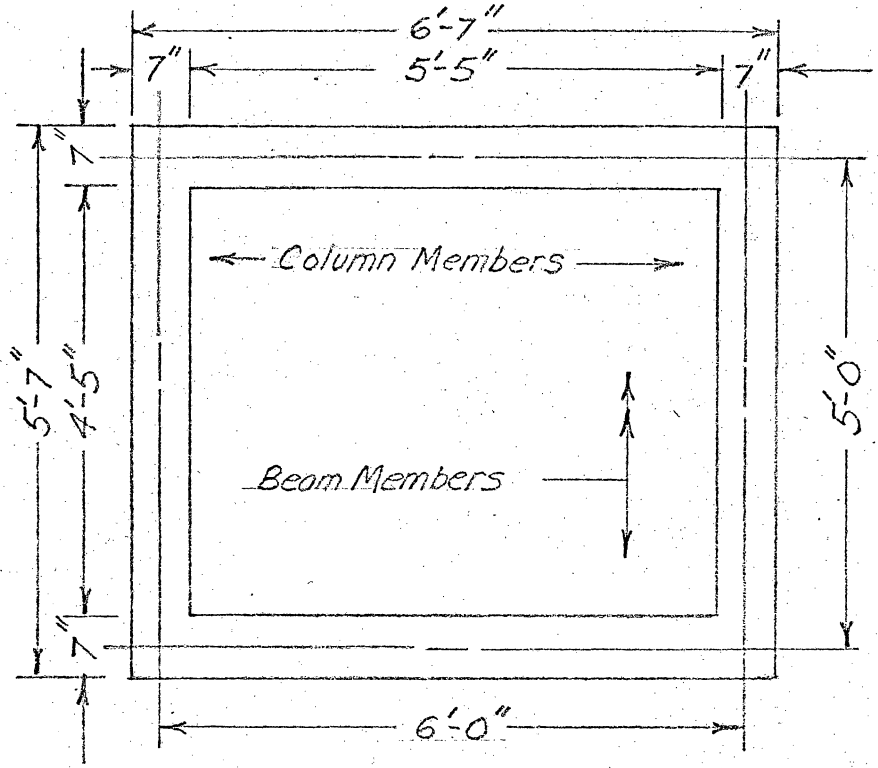

Figure 8a. Overall Dimensions of Frame

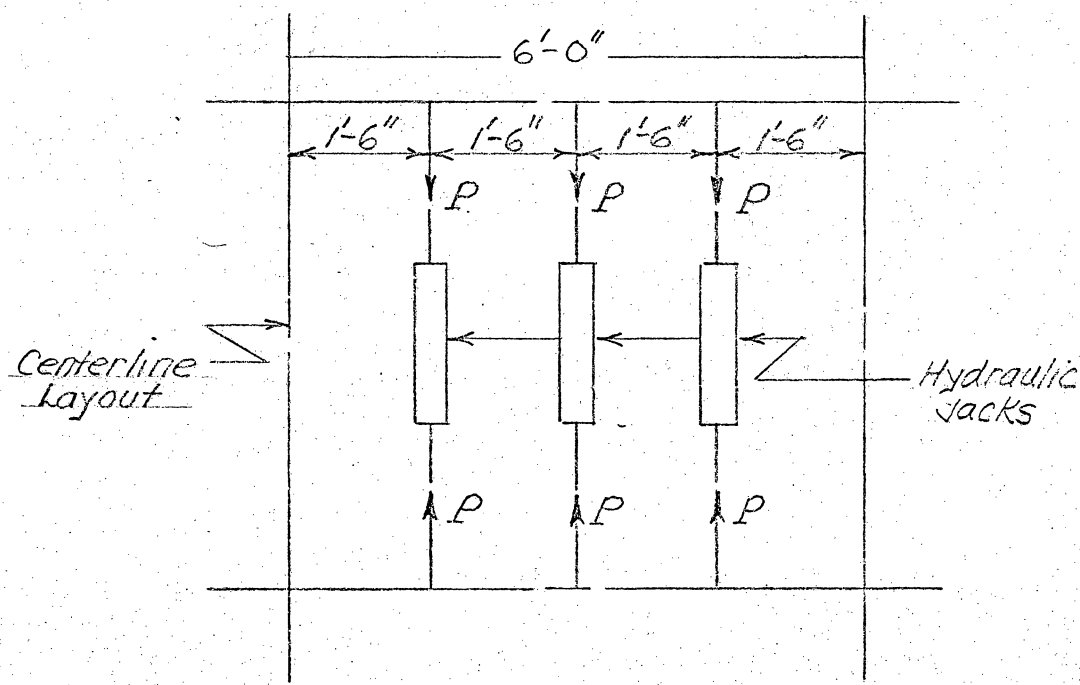

Figure 8b. Loading System

steel percentage ($p = A_s/bd$) would be less than p_{max} and the sections would be under reinforced. This was done, and the ultimate moment capacity (M_u) for the section, as defined by ACI 318-63 and omitting the capacity reduction factor, ϕ, was 6.960 FT-K. This ultimate moment is equated to the maximum moment found from an elastic moment distribution to give the ultimate load, P_u, for the section.

$$0.330\ PL = 6.960\ \text{FT-K}$$

$$0.330\ (6)\ P = 6.960$$

$$P_u = 3.52K$$

The beam sections, over the column supports, were reinforced with two No. 3 bars in the tension face. The ultimate moment, M_u, for the section was 4.100 FT-K. As before, this was equated to the maximum elastic moment for the section to give the ultimate load.

$$0.170\ PL = 4.100$$

$$0.170\ P(6) = 4.100$$

$$P_u = 4.02K$$

From the preceding information, the analytical prediction for the ultimate load for Frame No. 1 was, $P_u = 3.52K$.

The columns were designed for combined bending and axial load, with the value of 3.52K substituted for P in the loading system. The necessary reductions for slenderness effects were made, and lateral ties were provided as prescribed by the code. The structure was then reinforced for shear and diagonal tension, and checked for bond stresses and anchorage of reinforcing steel. Steel placement was carried out according to the code and the necessary concrete cover was provided. The final design, with reinforcement sizes and placement is shown in

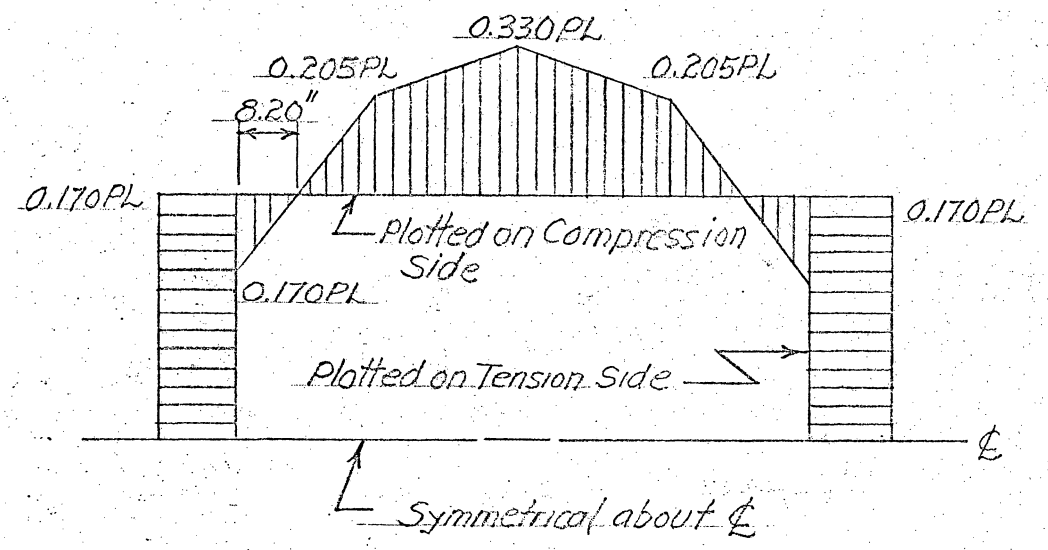

Figure 9. Elastic Moment Diagram - Frame No. 1

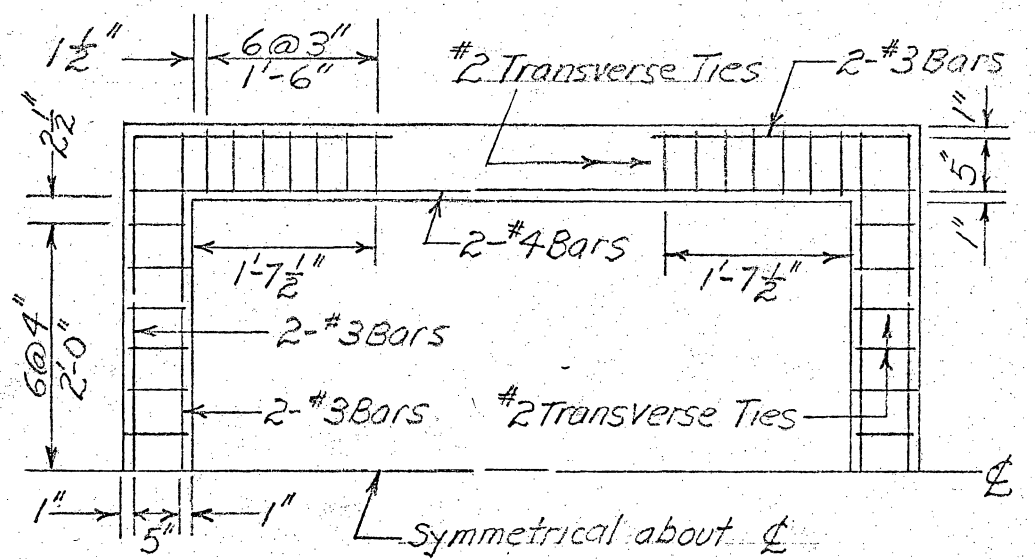

Figure 10. Final Design of Frame No. 1

Figure 10.

Frames No. 2 and No. 3 were analyzed by bilinear analysis with a "contaminated" region as proposed by Sawyer [17] and Rosenblueth and de Cossío [15], and by successive moment distribution, as proposed by Berwanger [4], using the perfect elasto-plastic moment-curvature curve.

Frame No. 2 was reinforced with two No. 4 bars tension reinforcement and two No. 4 bars compression reinforcement throughout the length of the beams. Transverse ties of No. 2 reinforcing steel were spaced at three inches and extended over the entire length of the beam members. The columns were reinforced with four No. 4 bars, and lateral ties of No. 2 reinforcing steel were spaced at four inches throughout the length of the columns. Frame No. 3 was reinforced exactly the same as Frame No. 2 with the exception that No. 3 reinforcing bars were used in place of the No. 4 bars.

The theoretical moment-curvature curves for Frames No. 2 and No. 3, using the bilinear approximation, are shown in Figure 11. The moment diagram and the curvature diagram are shown in Figure 12. The bending angles, equivalent to the areas of the curvature diagram, were balanced by equating the positive curvature area to the negative curvature area between the boundary points. The angle change from the centerline of the beam to the centerline of the column is zero; therefore, these points were taken as the boundary points, and the governing expressions for balancing the bending angles, as derived from statics, were:

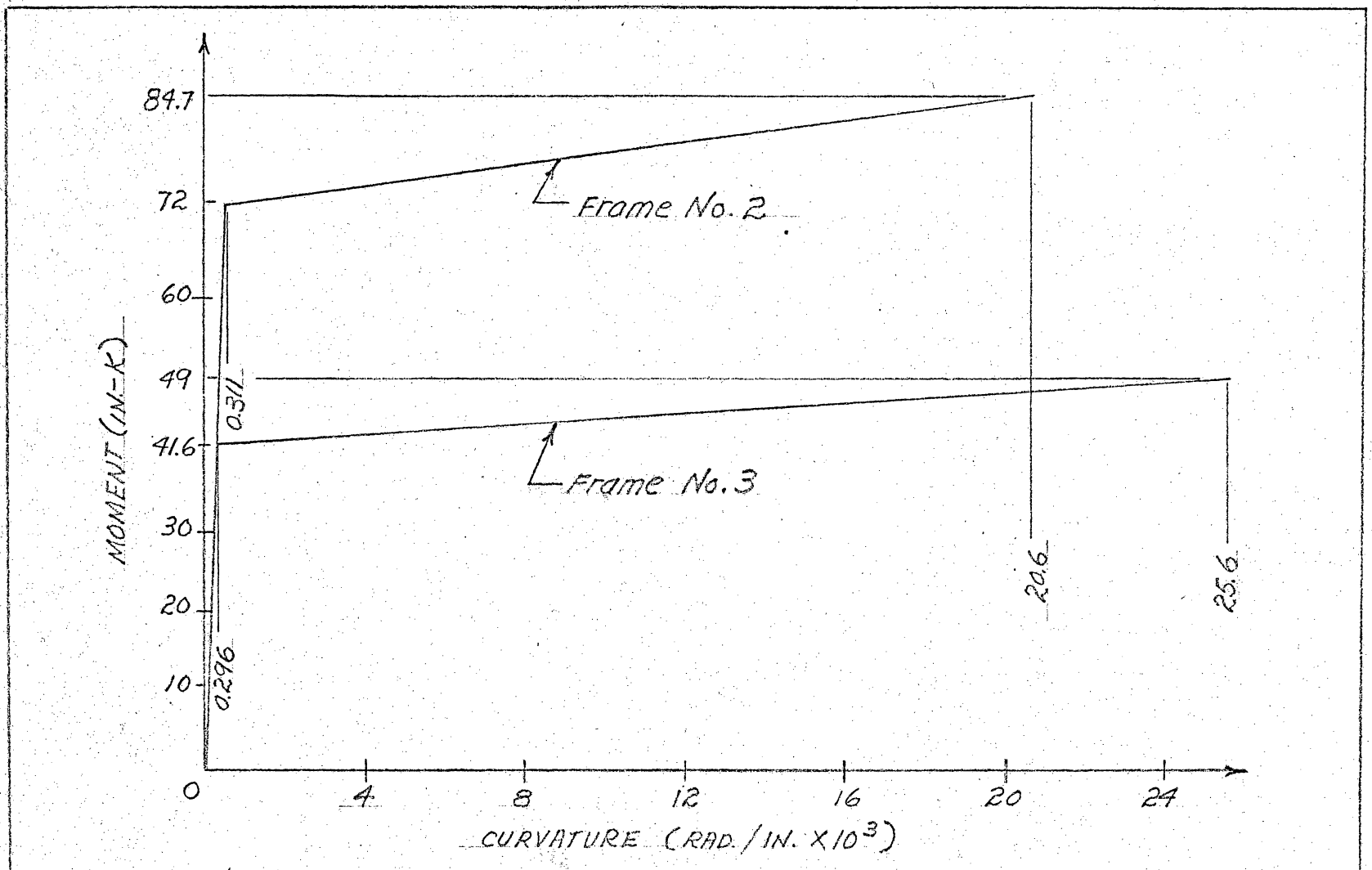

Figure 11. Theoretical Moment-Curvature Curves for Frames No. 2 and No. 3

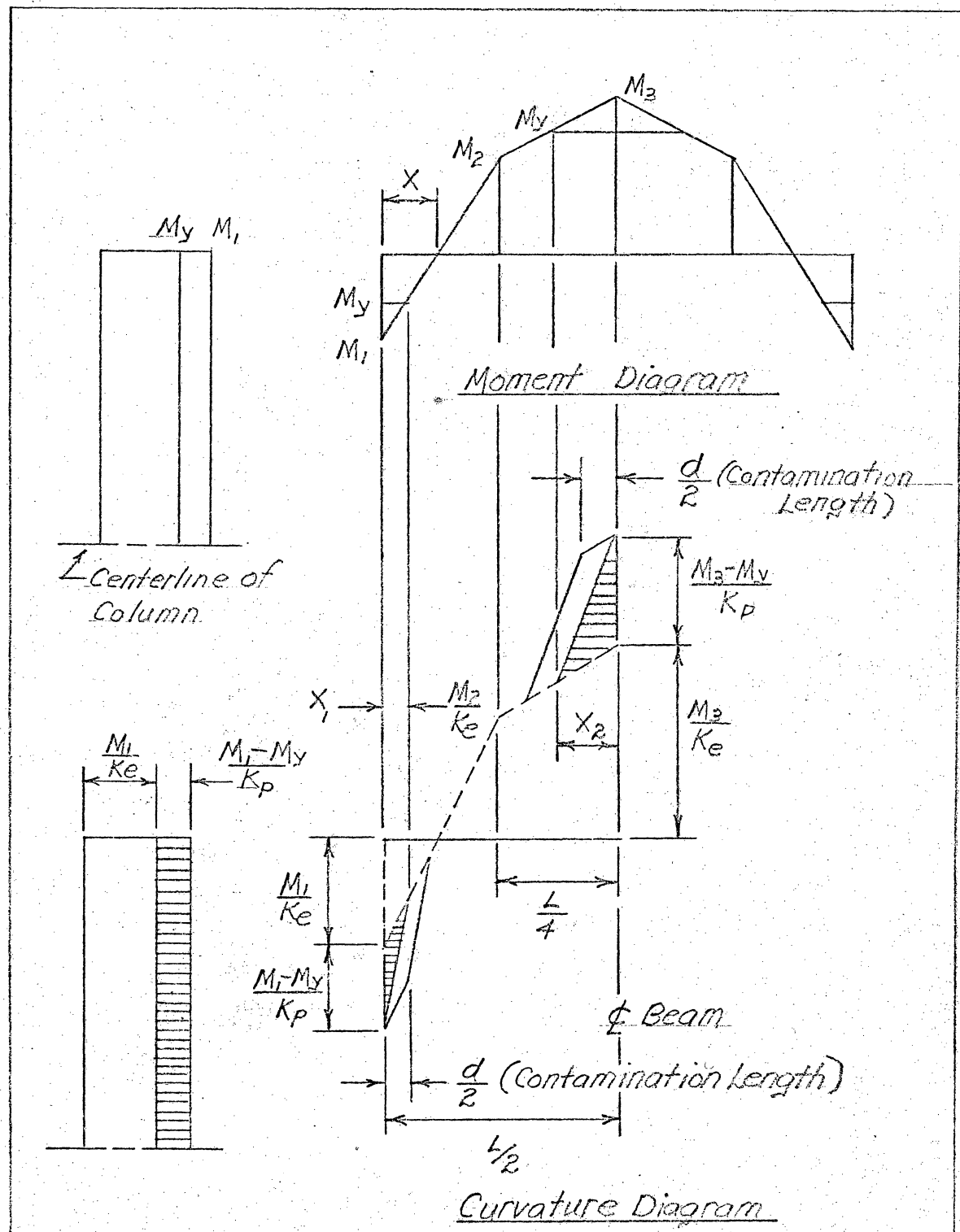

Figure 12. Moment and Curvature Diagrams - Bilinear

1. $M_3 - M_1 = 36P$
2. $M_2 - M_1 = 27P$
3. $X = 18M_1 / (M_1 + M_2)$
4. $X_1 = X - (M_y / M_1) X$
5. $X_2 = 18 (M_3 - M_y) / (M_3 - M_2)$
6. Positive curvature area = negative curvature area between boundary points.

M_3 was set equal to the ultimate moment, M_u, for the section as defined by ACI 318-63 without using the capacity reduction factor, ϕ. Then, a value of moment was assumed for M_1, and the positive and negative curvature areas computed. If there was a disagreement, another value for M_1 was assumed, and the procedure repeated until the agreement was attained.

The value of K_e ($E_c I$) was determined by using an I value for the transformed cracked section and an E_c value taken from the expression,

$$E_c = 57{,}500 \sqrt{f'_c}$$

The plasticity factor, k_p, was determined from the design charts given by Sawyer [17].

For Frame No. 2, the value of M_u or M_3 was 84.7 in-K, the value of M_e (0.85 M_u) was 72.0 in-K, and the value of M_1, that satisfied the boundary conditions, was 74.0 in-K. Thus,

$$M_3 - M_1 = 36P_u$$
$$84.7 - (-74.0) = 36P_u$$
$$P_u = 4.40K$$

For Frame No. 3, the value of M_u or M_3 was 49.0 in-K, the value

of M_e was 41.6 in-K, and the value of M_1, that satisfied the boundary conditions, was 42.9 in-K. Thus,

$$M_3 - M_1 = 36P_u$$
$$49.0 - (-42.9) = 36P_u$$
$$P_u = 2.55K$$

The final design for Frame No. 2 is shown in Figure 13.

Frames No. 2 and No. 3 were also analyzed by the successive moment distribution method proposed by Berwanger[4]. The moment diagram is shown in Figure 14. The first hinge forms at the center-line of the beam at a load, $P_1 = 2.92\ M_y / L$. An additional load of $1.08\ M_y / L$ produces hinges at the corners to form a collapse mechanism with an ultimate load, $P_u = 4.00\ M_y / L$. M_y is taken as 80% of the ultimate moment, M_u, defined by ACI 318-63.

For Frame No. 2, M_y ($0.80\ M_u$) was 67.8 in-K. Thus,

$$P_u = 4.00\ M_y / L$$
$$P_u = 4.00 \times 67.8 / 6 \times 12$$
$$P_u = 3.76K$$

For Frame No. 3, M_y ($0.80\ M_u$) was 39.2 in-K. Thus,

$$P_u = 4.00\ M_y / L$$
$$P_u = 4.00 \times 39.2 / 6 \times 12$$
$$P_u = 2.18K$$

It should be noted that the steel was placed in the corners differently in Frame No. 3. The compression steel, in the beam sections, near the supports, was not extended into the column supports. This was done to further reduce congestion over the supports, and save

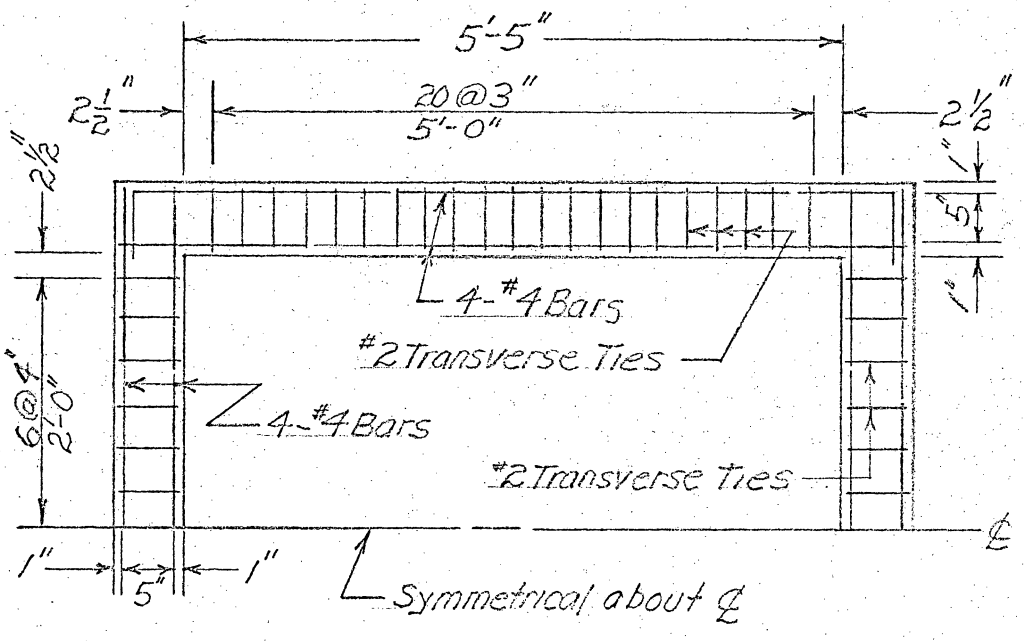

Figure 13. Final Design of Frame No. 2

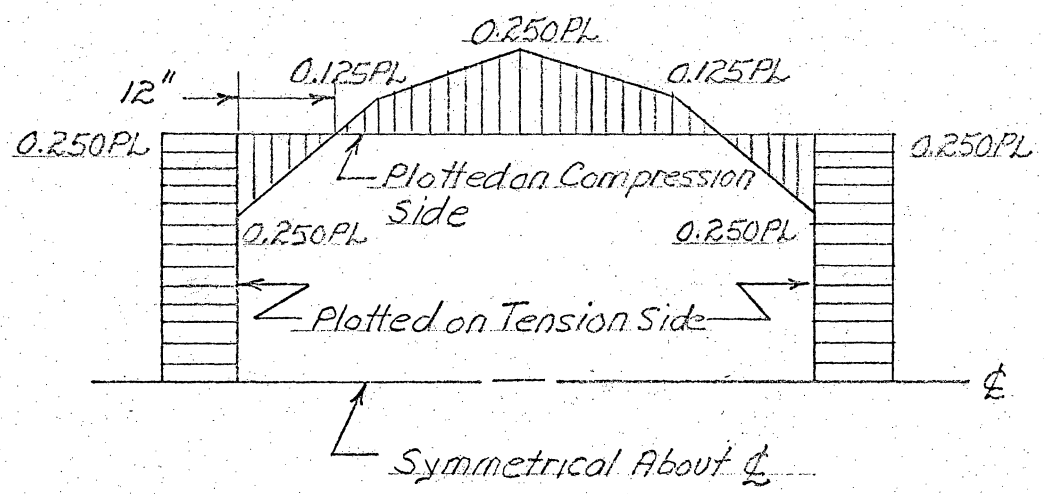

Figure 14. Moment Diagram from Successive Moment Distribution

bending of the bars in the columns. The ACI Code would never allow this practice; however, limit design allows for a reduction of reinforcement congestion at supports.

A summary of the frame designs and the predicted ultimate loads (P_u's) is given in Table 1.

TABLE 1

SUMMARY OF DESIGNS OF TEST FRAMES

	Frame No. 1		Frame No. 2		Frame No. 3	
	Beam Section	Corner Section	Beam Section	Corner Section	Beam Section	Corner Section
P	0.0167	0.0095	0.0167	0.0167	0.0095	0.0095
P'	0.0000	0.0167	0.0167	0.0167	0.0095	0.0095
q	0.2220	0.1780	0.2220	0.2220	0.1780	0.1780
q'	0.0000	0.2220	0.2220	0.2220	0.1780	0.1780
$q-q'$	0.2220	-0.0440	0.0000	0.0000	0.0000	0.0000
k_p	-	-	155	155	155	155
K_p	-	-	1500 $k\text{-in.}^2$	1500 $k\text{-in.}^2$	909 $k\text{-in.}^2$	909 $k\text{-in.}^2$
K_e	-	-	232,000 $k\text{-in.}^2$	232,000 $k\text{-in.}^2$	141,000 $k\text{-in.}^2$	141,000 $k\text{-in.}^2$
M_u	83.5 in-k	49.0 in-k	84.7 in-k	84.7 in-k	49.0 in-k	49.0 in-k
Elastic Ultimate Load, p_E	3.52K		3.53K		2.04K	
Limit Analysis p_L	3.50K		4.40K		2.55K	
Moment Dist. $p_{mom.-dis.}$	3.72K		3.76K		2.18K	

B. Experimental Program

Three frames were built and tested for the purpose of comparing test results with analytical predictions. Of secondary interest, was the effect that stirrups and compression steel have on the rotational capacity of reinforced concrete. The only variables for the frames were the reinforcing steel percentage (p) and the placement of the reinforcement.

The reinforcing steel consisted of ASTM-A-305 deformed intermediate grade steel. The stirrups were made of quarter-inch diameter, hot rolled, smooth bars. They were shaped in a bending device, fabricated in the shop, and welded at the joints. Reinforcing cages were tied with galvanized wire. Stress-strain curves for the steel used in the frames are shown in Figure 15. The yield stresses of the steel are given in Table 2 along with the other properties of the frames.

The concrete quantities were proportioned for a compressive strength of 3000 psi. The quantities, per cubic foot, used in the mix were:

Portland Cement (Type III)		19.4 pounds
Coarse Aggregate (1" maximum size)		63.5 pounds
Sand		55.8 pounds
Water	(approximately)	10.5 pounds

The concrete was mixed in a $3\frac{1}{2}$ cubic foot portable mixer. Each frame, with test cylinders, required three batches of concrete at two cubic feet per batch. Care was taken to obtain a desired consistency in concrete strength for each frame. Two test cylinders were taken from each batch of concrete, making a total of six per frame. Stress-

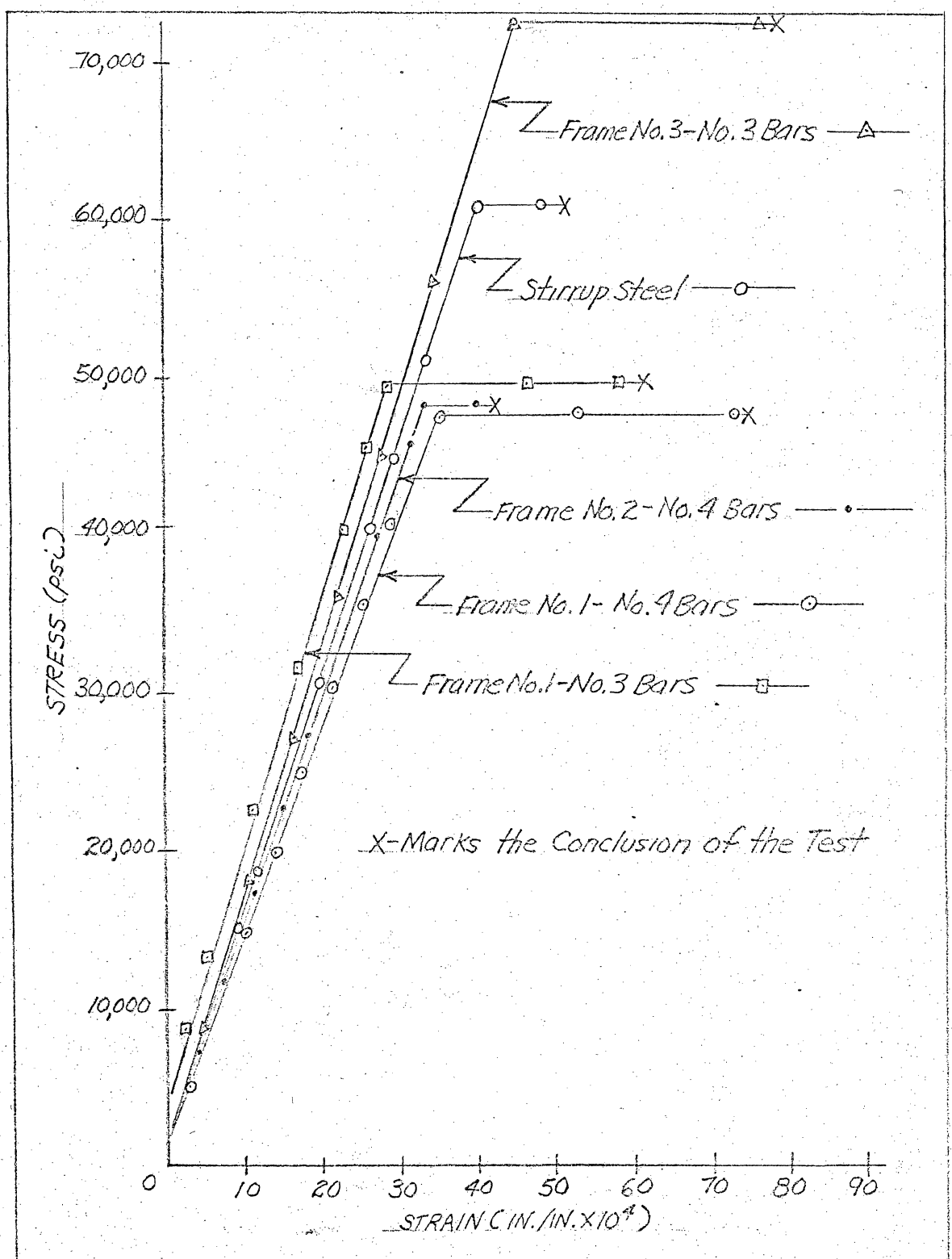

Figure 15. Stress-Strain Curves for the Reinforcing Steel

strain curves for the concrete used in each frame are shown in Figure 16. These curves were obtained by using a multiple regression computer program to obtain the best fitting curve for the stress-strain data obtained from compressive tests on the six test cylinders from each frame.

The frames were cast in forms made of 3/4" plywood finished on one side (A-C). The sides of the forms were braced with 2" x 4" blocks to hold the frame dimensions constant. The forms were varnished and oiled before the pouring of each test frame. This resulted in easy removal of forms after curing.

After the frames were poured, vibrated and finished, they were covered with wet burlap bags for curing. The bags were re-soaked each day and re-applied for four days thereafter. This was done because of the size and location of the frames. On the seventh day, the frames were removed from the forms and placed in a horizontal position, on four one-inch diameter ball bearings resting on 2" x 4" blocks at each of the four corners of the frame. The instrumentation was applied and the frames were made ready for testing the next day. The concrete test cylinders were handled in exactly the same manner, and were tested the same day as the frames. The concrete compressive strengths are given in Table 2.

The instrumentation consisted of strain measuring devices applied at the assumed hinging regions, and dial gages for measuring various deflections. Strains were determined by measuring the relative increases or decreases in the distance between two fixed points in a line parallel

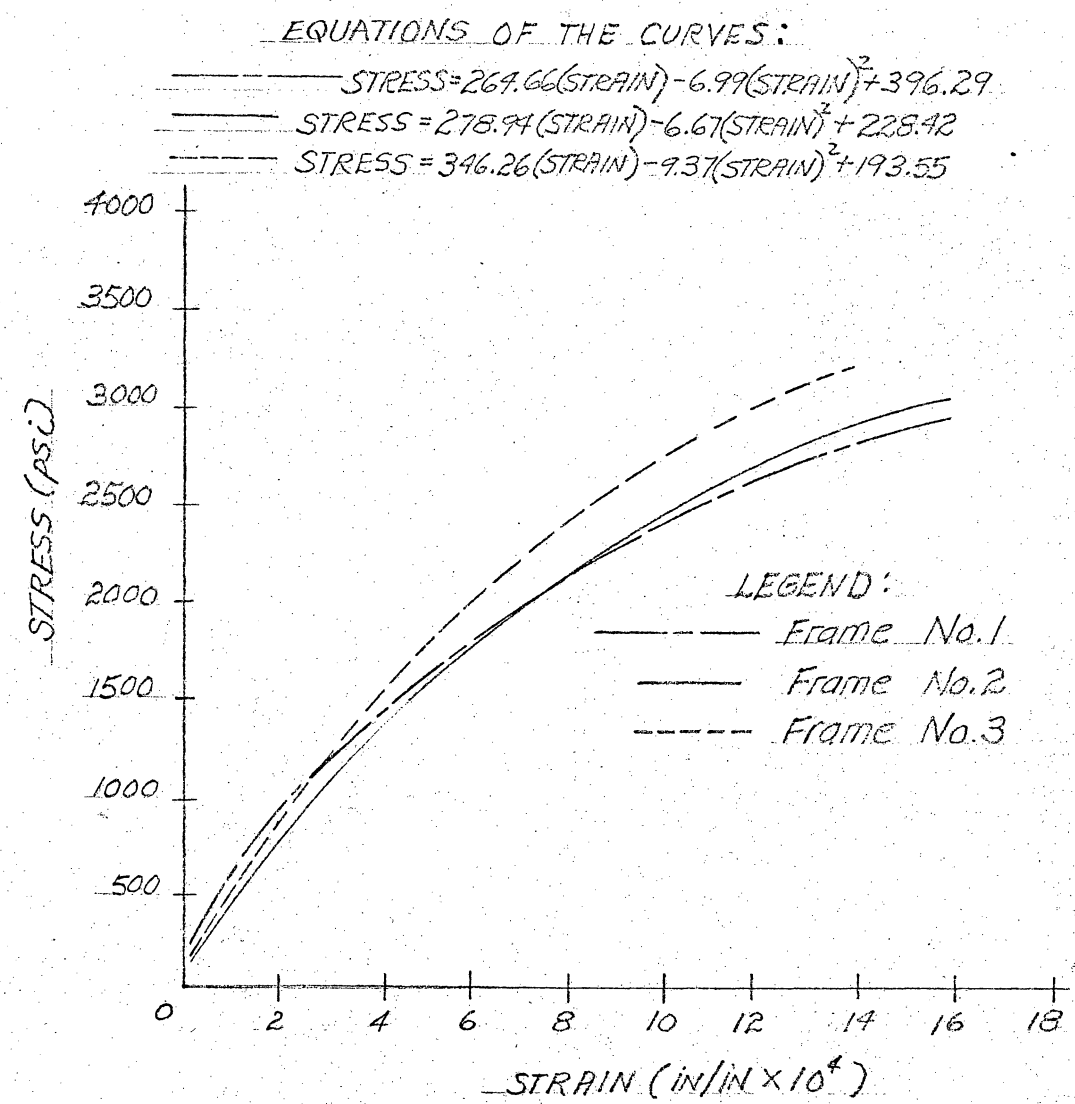

ULTIMATE STRESSES:

FRAME No.1 — $f_c' = 2900$ psi

FRAME No.2 — $f_c' = 3000$ psi

FRAME No.3 — $f_c' = 3190$ psi

Figure 16. Statistical Stress-Strain Curves for the Concrete

TABLE 2

Properties of the Test Frames

Property	Frame No. 1	Frame No. 2	Frame No. 3
Effective Depth of Beams (d)	5.375 in.	5.750 in.	5.875 in.
Tension Steel at Center of Beams	2- #4 Bars $A_s = 0.40$ in.^{2}	2- #4 Bars $A_s = 0.40$ in.^{2}	2- #3 Bars $A_s = 0.22$ in.^{2}
Compression Steel at Center of Beams	———	2- #4 Bars $A_s' = 0.40$ in.^{2}	2- #3 Bars $A_s' = 0.22$ in.^{2}
Tension Steel at Corners	2- #3 Bars $A_s = 0.22$ in.^{2}	2- #4 Bars $A_s = 0.40$ in.^{2}	2- #3 Bars $A_s = 0.22$ in.^{2}
Compression Steel at Corners	2- #4 Bars $A_s' = 0.40$ in.^{2}	2- #4 Bars $A_s' = 0.40$ in.^{2}	2- #3 Bars $A_s' = 0.22$ in.^{2}
Steel in Columns	4- #3 Bars $A_{st} = 0.44$ in.^{2}	4- #4 Bars $A_{st} = 0.80$ in.^{2}	4- #3 Bars $A_{st} = 0.44$ in.^{2}
Concrete Strength	2900 psi	3000 psi	3190 psi
Steel Yield Stress	No. 4 - 48.0 ksi No. 3 - 49.6 ksi	48.3 ksi	74.0 ksi
Yield Stress of Stirrups	61.3 ksi	61.3 ksi	61.3 ksi

to the longitudinal axis of the member. The relative increases or decreases in distance were measured by a gage, which worked in a manner similar to a mechanical extensiometer. Rotations were determined from a knowledge of the strain at the top and bottom of the member. A line perpendicular to the longitudinal axis of the member defines a zero strain line. The angle that the actual strain line makes with the zero strain line gives the rotation of that section of the member.

The "fixed points" were acquired by forming special brass inserts into the concrete where strain readings were desired. The plugs were placed into the concrete, at a fixed distance of 10 inches apart, by an aluminum template. The plugs were screwed to the template before application. Before testing, the templates were removed and the plugs were capped with special inserts that had a 1/32 inch "seat" for the points on the strain measuring device. The measuring of strains by this system was accurate to within $\pm$ 0.002 inches. This was sufficient since the strains sometimes were as large as 0.50 inches. The locations of the strain points on the frames are shown in Figure 17. The points at the top and bottom coincided with the longitudinal axes of the compression and tension steel.

The loads were applied to the frames by three hydraulic jacks which were strapped to the beam members. The jacks pulled the beam members toward each other, placing the columns in combined bending and axial compression, in the same geometric plane as the centerlines of the frame. This insured against any torsion in the frame members.

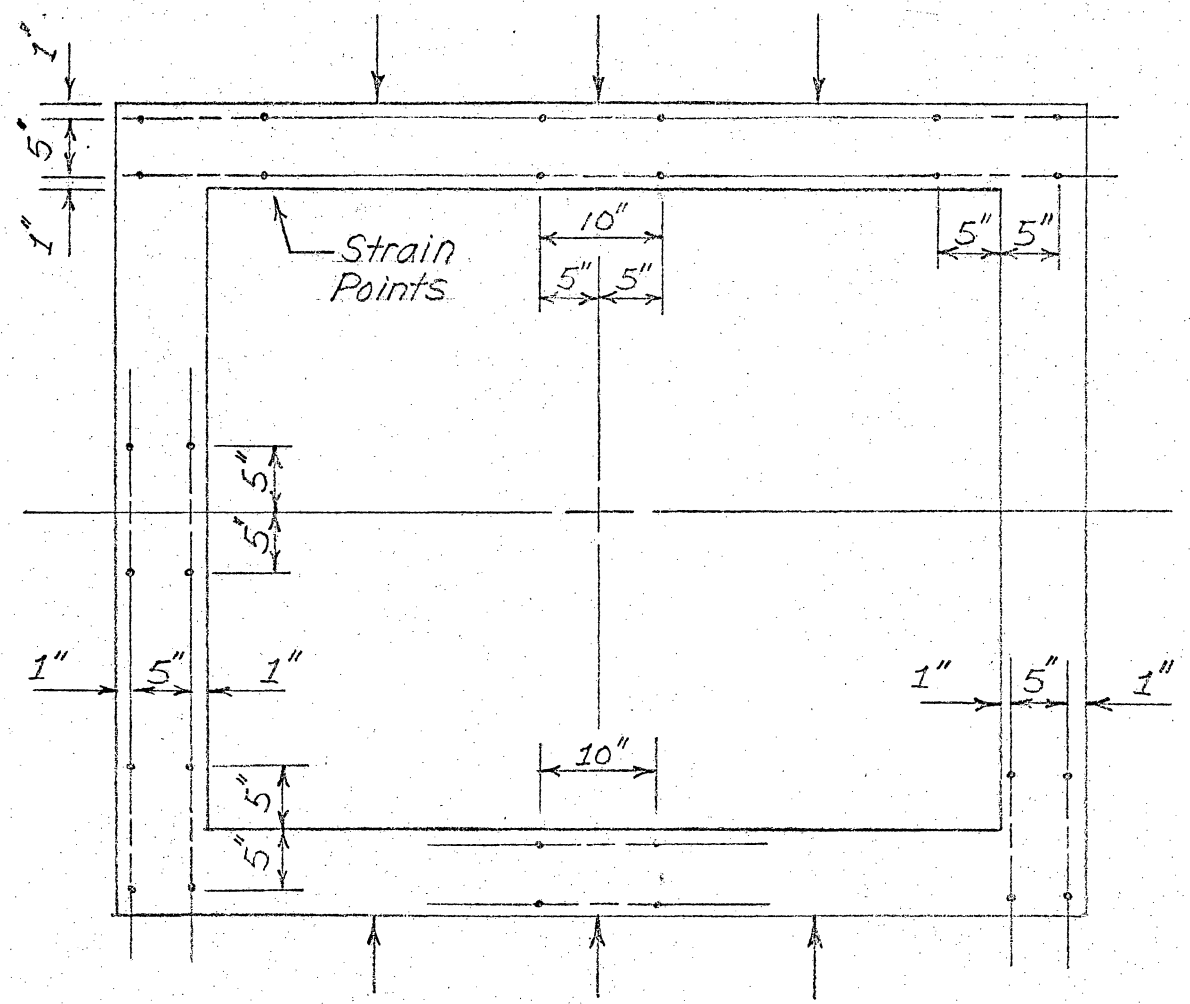

Figure 17. Location of Strain Points on Frames

The jacks were connected to the beams by a strap and clevice arrangement shown in Figure 18. The straps and clevices were made from 4 inch x $\frac{1}{4}$ inch and 4 inch x $\frac{1}{2}$ inch cold-rolled, mild steel plates. They were fabricated in the Engineering Mechanics Shop, and were designed for the straps to fit snugly over the members and the clevices to be connected to the straps with $\frac{1}{2}$ inch diameter hex-head bolts. The jacks were then connected to the clevices by 5/8 inch diameter hex-head bolts.

Three jacks, which were known to have very nearly the same size pistons, were selected and calibrated using a standard testing machine. The pressure vs. load curves were determined, and the jacks were found to be equal in piston size. A linear regression was made on the pressure-load data from all three jacks to determine the best fitting pressure-load relationship. This curve is shown in Figure 19.

The jacks were connected at the quarter points of the beam members, 1' 6" apart. They were then hooked to the same pressure line and the load applied was determined from the line pressure by using the calibration curve.

A five horsepower electric motor powered a three gallon-per-minute pump which applied pressure to the jacks. The pump and motor were mounted on a stand along with the necessary pressure gages and valves for regulating the pressure applied.

The tests were started in the morning and ran for approximately seven hours. An initial load was applied followed by four incremental loadings at 15 percent of the predicted ultimate load, P_u, eight

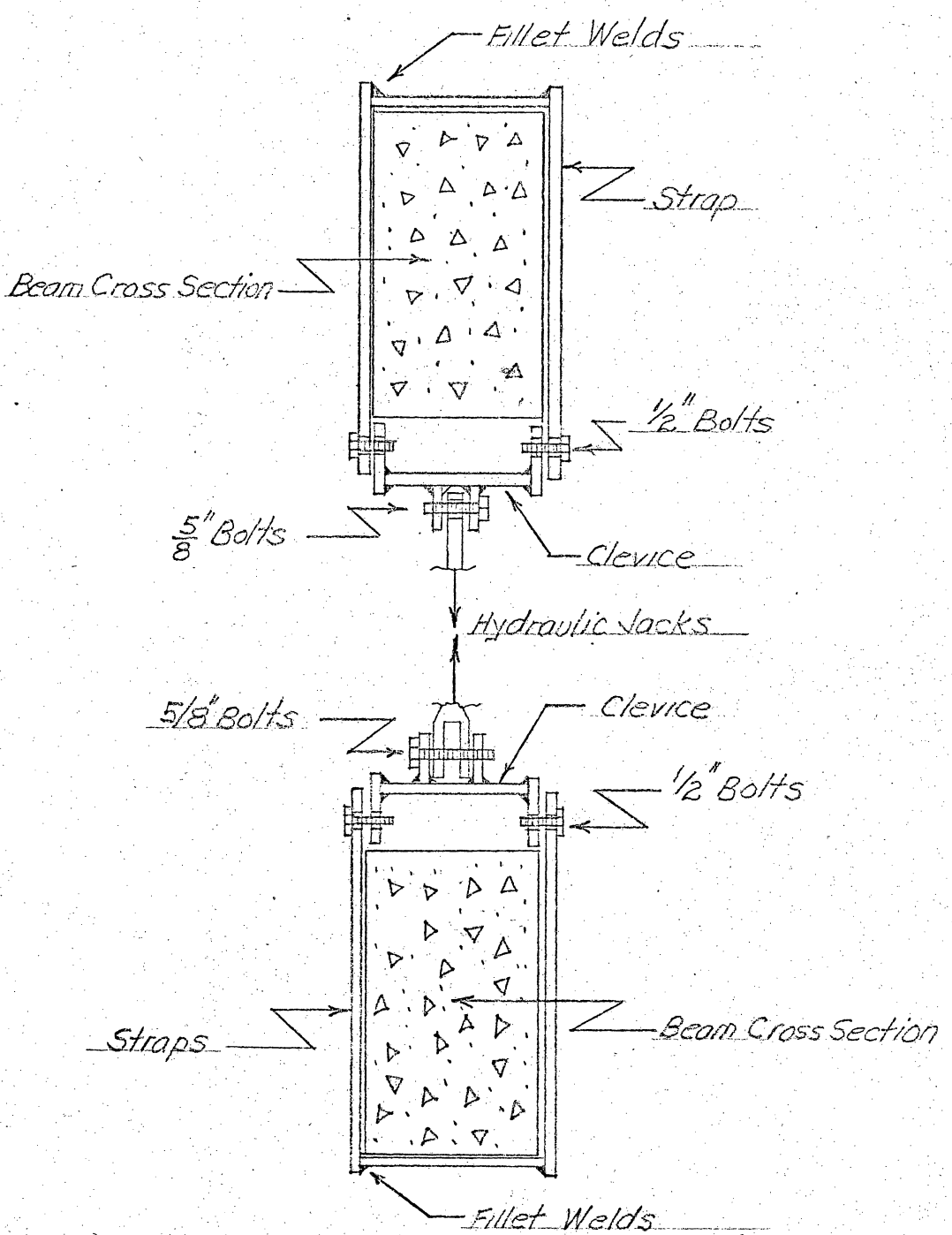

Figure 18. Straps and Clevices in Loading System

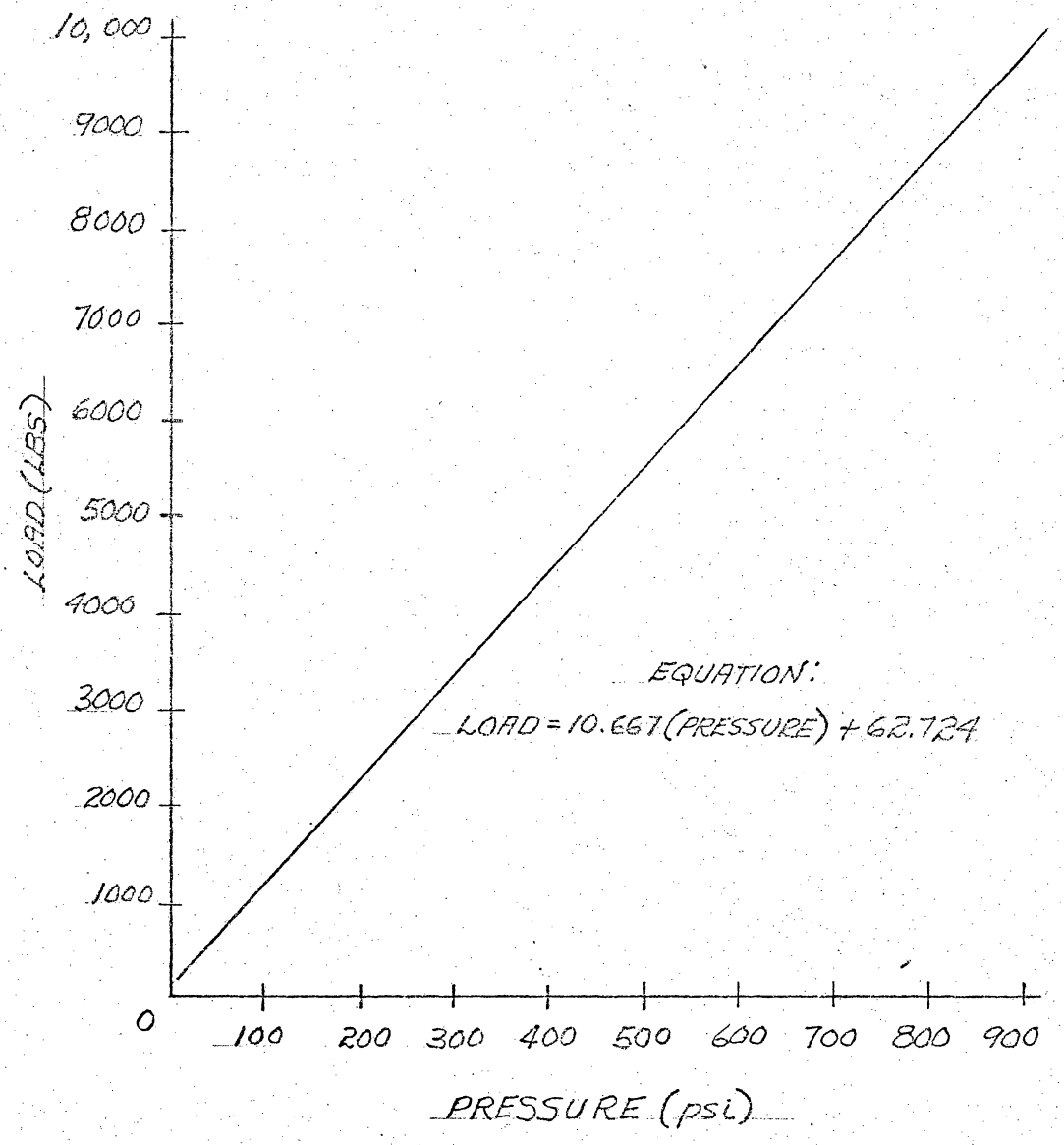

Figure 19. Load-Pressure Calibration Curve for Hydraulic Jacks

incremental loadings at five percent of P_u, and the remaining incremental loadings, after yield, of 0.200 inches centerline deflection of the beams. There was an elapsed time of 15 minutes to allow the system to reach equilibrium for each of the loading increments.

Figure 20 shows the complete test setup.

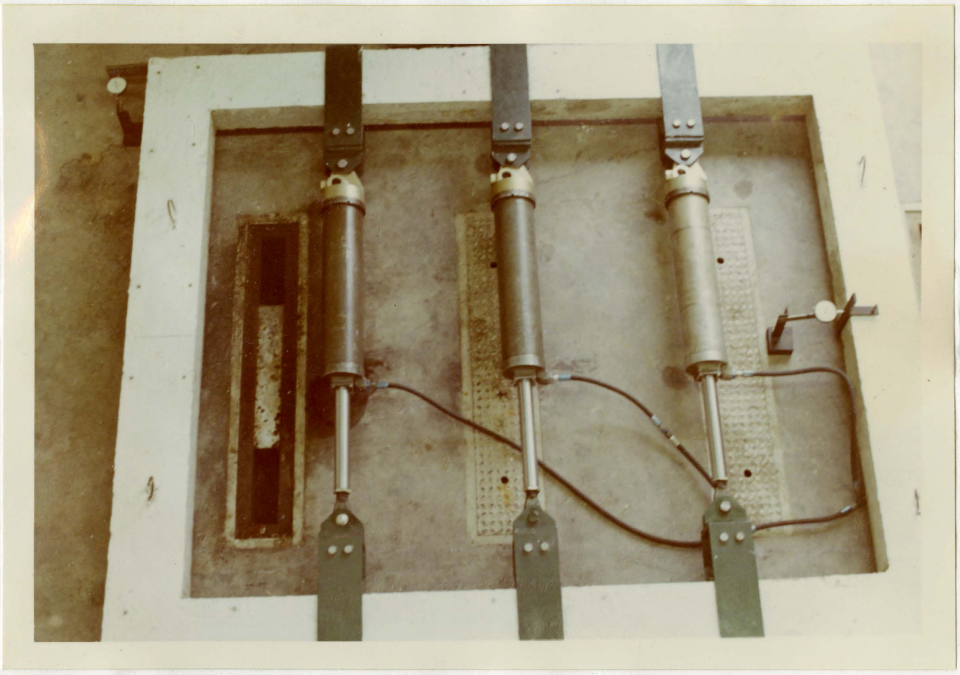

Figure 20. The Complete Test Setup

C. Test Results

All three frames behaved similarly under loading in the elastic range. Hairline cracks were first observed at a load of approximately 75% of the ultimate load. The cracks formed in the tension area at the midspans of the beams and the exterior faces of the columns. As the load increased, the cracks extended in length toward the compression regions of the members. The cracks at the midspans of the beams were slightly inclined toward the center portion of the beams, indicating the presence of diagonal tension stresses.

There were three possible collapse mechanisms that could form in the frames; these are shown in Figure 21.

Yielding occurred initially at the midspans of the beams in Frame No. 1. However, the moment redistribution from the midspans to the corners proved unsymmetrical, and at the ultimate load of 4.60K, sidesway was initiated in the frame and wide tension cracks formed in diagonal corners of the frame at the ends of the columns. The cracks spread across the columns at approximately a 45° angle toward the interior faces of the columns directly adjacent to the beams. Figure 22 best describes this corner failure pattern.

The frame took on the collapse mechanism shown in Figure 21(a) with hinges forming at diagonal corners and the midspans of the beams at an ultimate load, P_u, of 4.60K. All sections failed in compression. The load dropped at the rate of approximately 0.3K every 15 minutes after ultimate, and the test was concluded with the frame completely "unserviceable", but continuing to hold a load of 3.3K. Figure 23

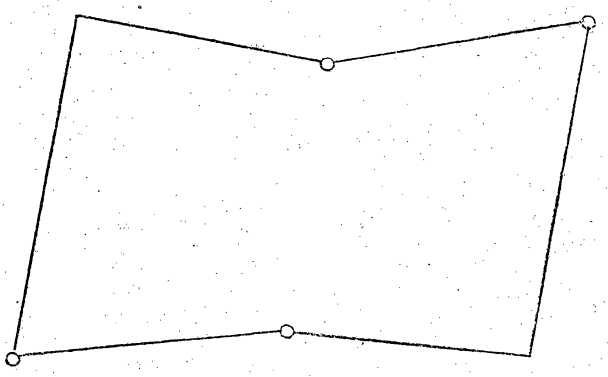

(a)

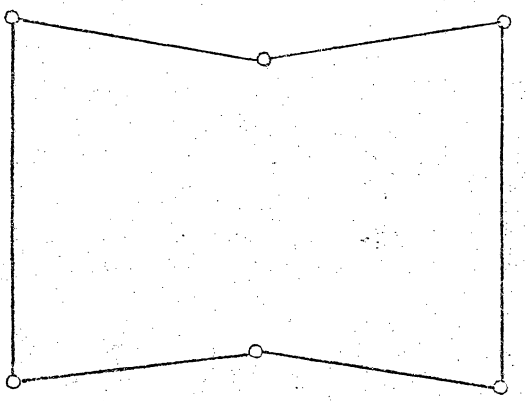

(b)

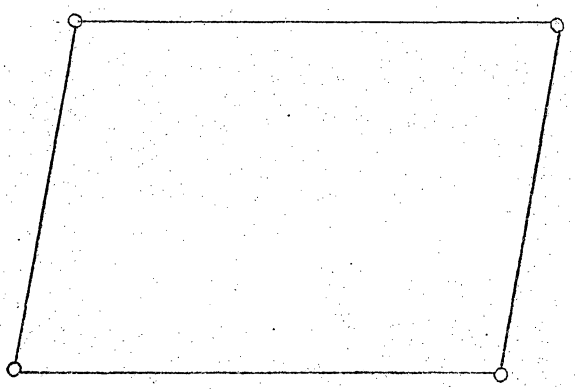

(c)

Figure 21. Possible Collapse Mechanisms for the Frames

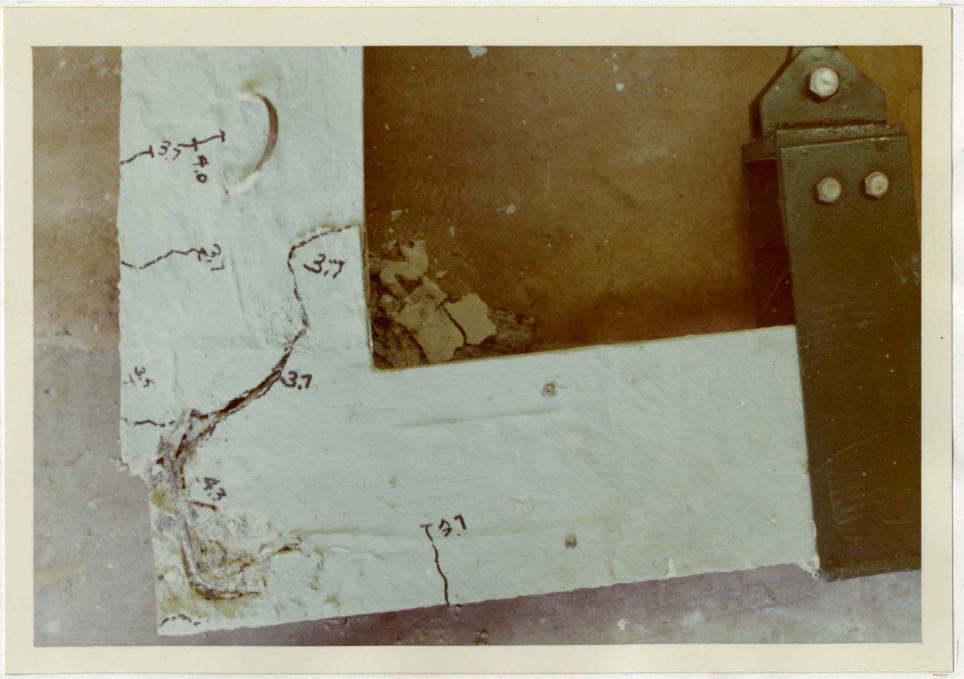

Figure 22. Corner Failure Pattern of Frame No. 1

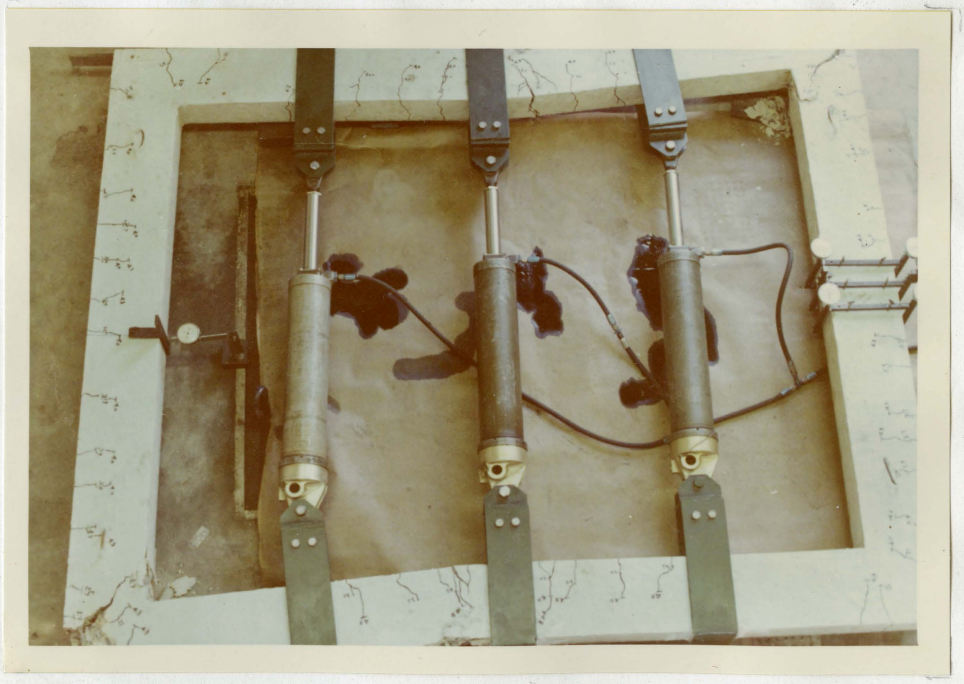

Figure 23. Total Collapse of Frame No. 1

shows the total collapsed frame with the sidesway clearly visible.

In Frame No. 2, yielding occurred initially in the midspan of only one of the beam members. Moment redistribution proved symmetrical, and the yielding center section rotated enough to allow hinges to form at the column supports to the left and right of the center section. However, the other two corners of the frame and the midspan of the other beam did not reach yielding.

The collapse mechanism was a beam mechanism, shown in Figure 21(b), with hinges forming at the midspan of the beam and the adjacent two corners. The corner failure pattern as shown in Figure 24 was very similar to that of Frame No. 1. Wide cracks formed in the exterior faces of the columns at a point where the steel in the columns was bent in to allow the compression steel in the beams to extend through. Figure 25 shows the steel placement in the corner. This reduced the effective depth of steel in the columns and explains why the ultimate load, P_u, for Frame No. 2 of 4.33K was less than the P_u for Frame No. 1. Figure 26 best describes the total collapse of Frame No. 2.

Frame No. 3, as mentioned previously, was reinforced so that the compression steel did not extend into the column supports, thereby avoiding the bending of the steel in the columns. As a consequence, a premature failure occurred over one of the column supports. The failure was apparently caused by a combination of shear and bond stresses. The frame held an ultimate load, P_u, of 3.74K. After ultimate, the load dropped rapidly to a value of 2.84K, and upon reapplying load, a sudden failure occurred with the complete separation of the

Figure 24. Corner Failure Pattern of Frame No. 2

Figure 25. Steel Placement in Corner of Frame No. 2

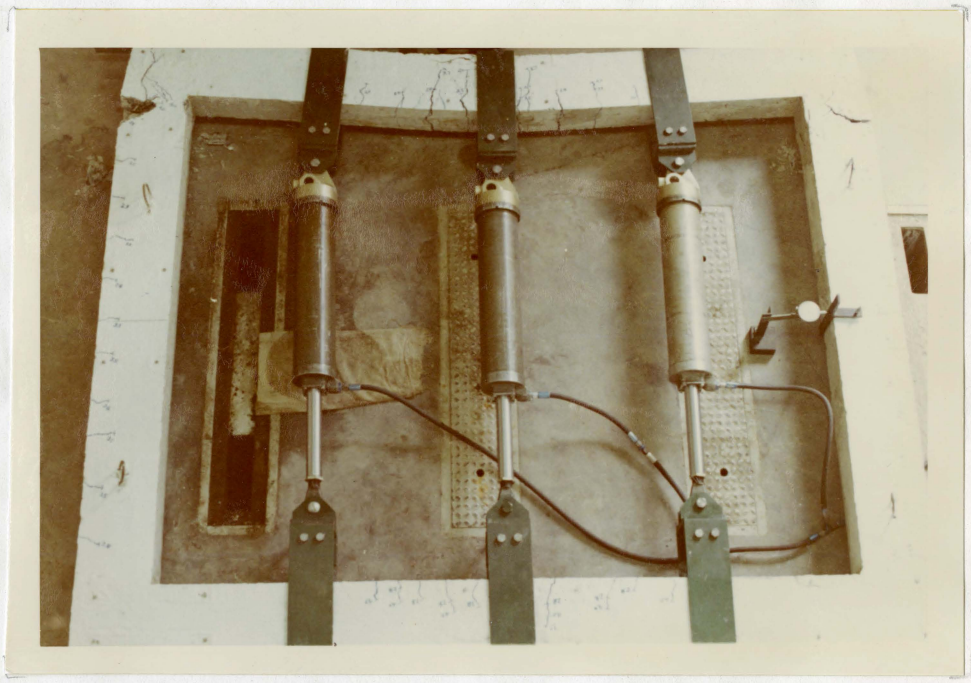

Figure 26. Total Collapse of Frame No. 2

beam member from the column at one corner of the frame. This is shown in Figure 27.

The data from the tests were fed into a computer program shown in Appendix C. The program reduced the data to values of load, rotation, depth to neutral axis, and concrete strain shown in Tables 4-13 given in Appendix A. The load-deflection data are shown in Tables 14-16 given in Appendix B.

Table 3 on page 56 gives a comparison of the predicted ultimate loads, arrived at by the various analysis techniques, and the actual ultimate loads that the frames carried. Ratios of the actual ultimate load to the predicted ultimate load are also shown in the table.

Figure 28 gives a comparison between the actual load-rotation curve and the predicted load-rotation curve for Frame No. 2. The X marks the conclusion of the test.

Figure 29 gives a comparison between the load-rotation curves for the cross sections at the midspans of the beams in Frames No. 1 and No. 2 and load-rotation curves for the same two cross sections at the midspans of two simple beams under a concentrated load at the midpoints. The data for the simple beams were obtained from previous laboratory tests conducted by the writer and his colleagues.

Figure 30 shows the load-rotation curves for the column supports for Frames No. 2 and No. 3.

Figure 27. Premature Failure in the Corner of Frame No. 3

TABLE 3

COMPARISON OF THE PREDICTED ULTIMATE LOADS WITH THE ACTUAL ULTIMATE LOADS

	Actual Ultimate Load $P_{Act.}$	Elastic Predicted Ultimate Load, P_E	Bilinear Analysis Ultimate Load, P_{Limit}	Successive Moment Distribution Load, $P_{Mom.-Dist.}$	$\frac{P_{Act.}}{P_E}$	$\frac{P_{Act.}}{P_{Limit}}$	$\frac{P_{Act.}}{P_{Mom.-Dist.}}$
Frame No. 1	4.60K	3.52K	3.50K	3.72K	1.31	1.32	1.24
Frame No. 2	4.33K	3.53K	4.00K*	3.76K	1.23	1.08	1.15
Frame No. 3	3.74K	2.04K	2.55K	2.18K	1.83	1.47	1.72

* Taking into account the reduced effective depth in the columns

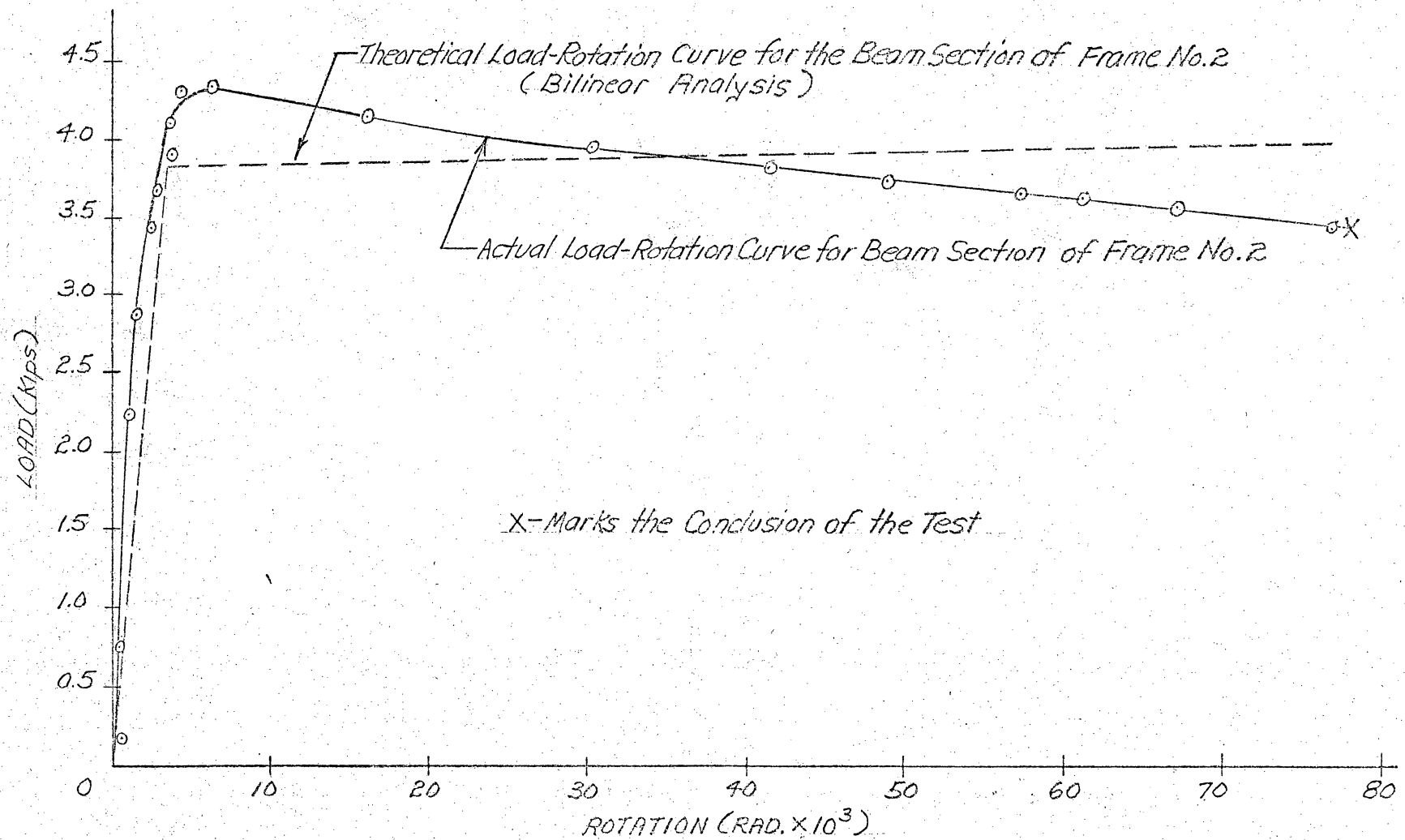

Figure 28. Comparison Between the Actual and the Theoretical Load-Rotation Curves

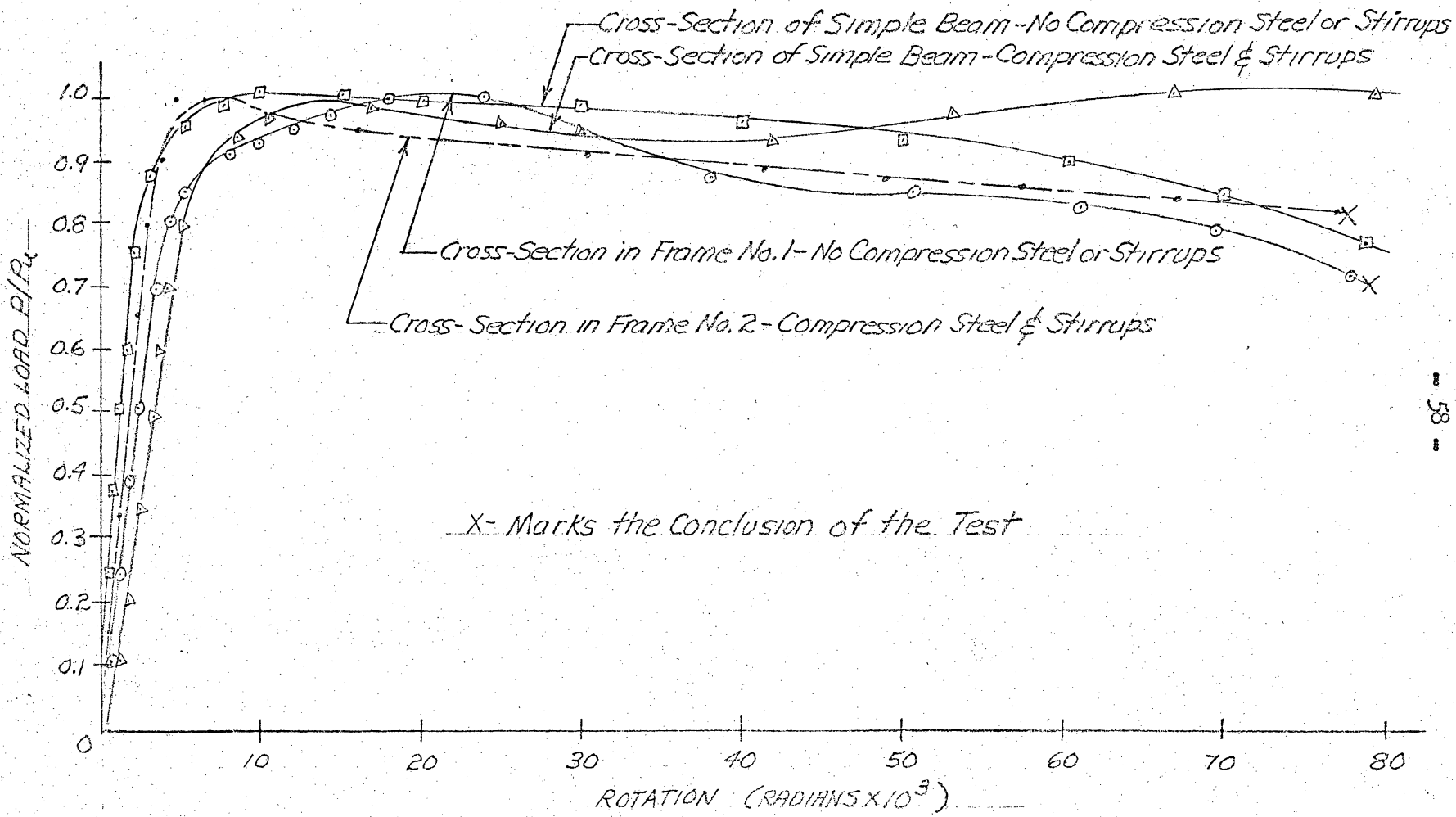

Figure 29. Comparison Between Load-Rotation Curves for Simple Beams With Those of Frames

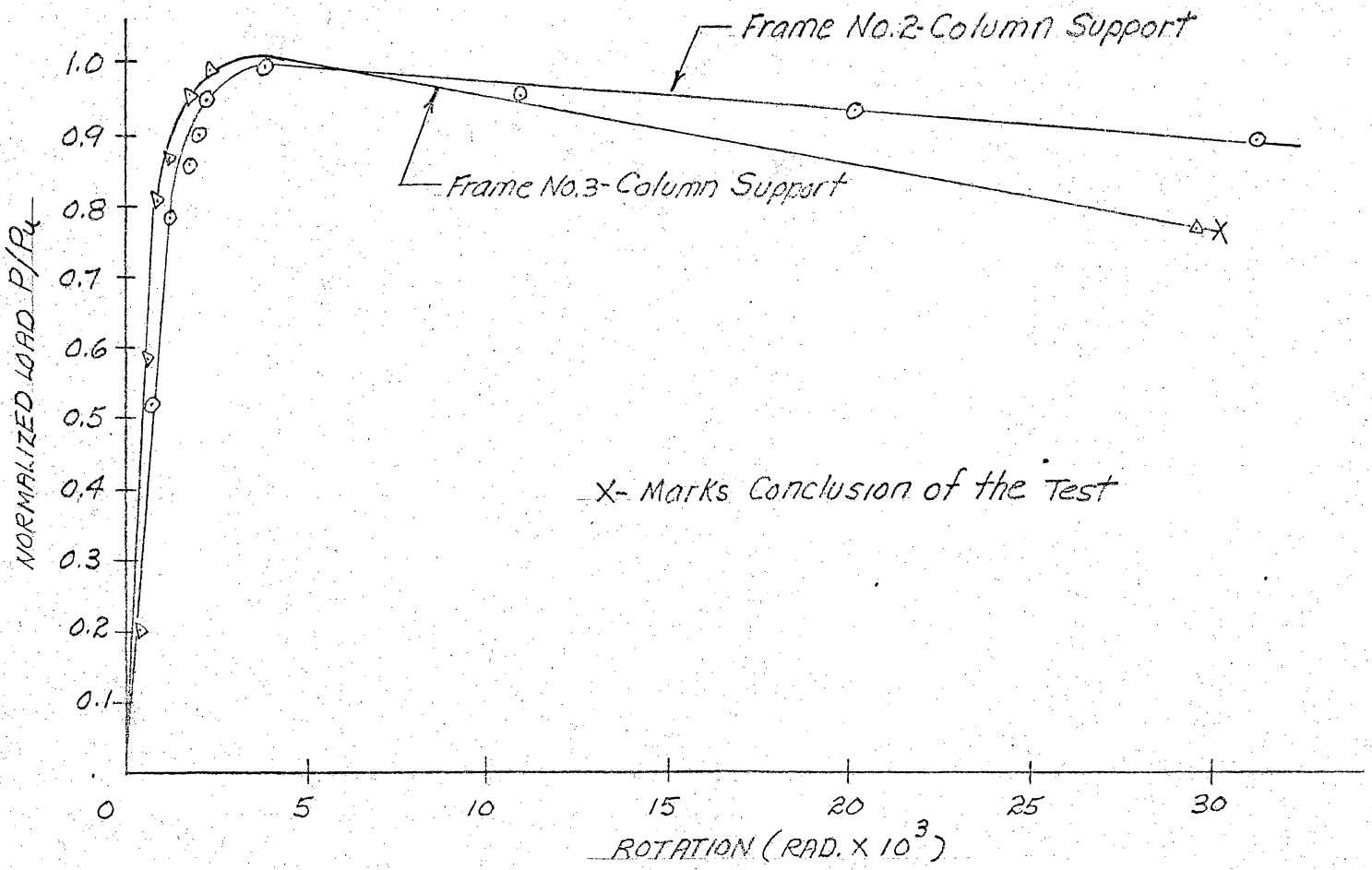

Figure 30. Load-Rotation Curves for Frames No. 2 and No. 3 at the Supports

IV. DISCUSSION

The primary objective of this investigation was to compare experimental test results with analytical predictions which were determined by using both an elastic analysis and a limit analysis. Since there was no simple way of determining the moments at the critical sections of the frames experimentally, the actual ultimate loads which the frames carried were compared with the theoretical predictions for ultimate loads. This comparison is limited in value since it is a well known fact that in an indeterminate structure, the load could very well be increasing while the moment at a particular section could be decreasing. On the other hand, the load could be decreasing due to a failure at one section while the ultimate moment at another section had not been reached. Thus, a knowledge of the moments at the critical sections is greatly missed in this investigation. However, it is felt that a comparison of predicted ultimate loads with the actual ultimate loads is of value in determining which method of analysis comes the closest to accurately predicting the flexural behavior of reinforced concrete frames.

Looking closely at Table 3, it can be seen that the ratio of the actual ultimate load to the predicted ultimate load in all cases is greater than 1.00. However, in general, the limit analysis predictions were closer to the actual load carrying capacities of the frames than the elastic predictions. But, the limit analysis predictions were still conservative, and in the case of Frame No. 3 were greater than 50% too low. For Frame No. 1, the analytical predictions of both the

elastic analysis and the limit analysis were 30% too small.

There are several explanations for the discrepancies between the predicted and the actual ultimate loads. The ACI Code's equation for ultimate moment capacity was used in all cases for determining M_u at the critical sections. In this equation, the value of M_u is seen to depend directly upon the yield stress of the steel, f_y. In Frame No. 1, the steel stress at the support section was approximately 63 ksi. The yield stress for the steel was 49.6 ksi, indicating that the steel probably was in the strain hardening region. Thus, the ACI Code equation does not take into account the strain hardening property of steel and is a conservative estimate of the ultimate moment capacity for reinforced concrete.

Also, in the case of Frame No. 1, the slope of the "plastic" portion of the bilinear curve for the corner section was so small that additional rotation area (area under the curve) resulted in only a slight increase in moment. If the descending branch of the moment curvature curve had been used at the center section where there was a definite spread of contamination, then additional rotational capacity would have been provided at the center section along with a corresponding increase in predicted moment at the corner section.

Examining the load-rotation data given in Tables 4-13 in the form of values of load, rotation, depth to neutral axis, and concrete strain at the extreme compressive fibers, there are several factors of interest to be noted.

In the elastic region at very low values of load, there are some negative values of the neutral axis depth and some decreases in

succeeding values of rotation. These are unreasonable and the errors can be attributed to the inability of the strain measuring device to detect very small increments in strain at the critical sections. All the values (rotation, depth to neutral axis, and concrete strain) depend on the strain readings and are therefore inaccurate at low values of load.

The experimental values of depth to neutral axis at ultimate load compare favorably to the values computed using equations from ACI Code 318-63 and assuming a rectangular concrete stress block with a maximum stress of 0.85 f_c' and a maximum strain of 0.003 in/in. The experimental values of neutral axis depth decrease slightly as the ultimate load is reached. At ultimate load, the values are somewhat larger than the computed values indicating that the concrete strain was higher than the value of 0.003 in/in used in computing the neutral axis depth.

The experimental values of concrete strain at which crushing and spalling occurred were as high as 0.007 in/in. This is a 130% increase above the ultimate concrete strain of 0.003 in/in given by ACI 318-63 in Section 1503(c). The increase may be accounted for by the closely spaced transverse ties and compression steel which "bind" the concrete in the reinforcement cage. The lateral ties upon being distressed, create a triaxial compressive stress in the concrete which increases the deformation capacity. This finding leads to the conclusion that the stress-strain curve for concrete determined from a standard compression test is not an accurate representation of the

behavior of the same concrete in a structural member under a different state of stress.

Another important point which merits discussion concerns the idea of using load-deformation relationships for cross sections of simple beams to represent the behavior of the same sections in indeterminate continuous beams and frames. Figure 29 shows the non-dimensional load-rotation curves for the cross sections at the midspans of the beams in Frames No. 1 and No. 2 and for the same cross sections in two simple beams under a concentrated load at the midspans. Noticing the curves for the sections in the simple beams, one can see that the section with compression steel and transverse ties is more ductile than the section with only tension reinforcement. However, observing the curves for the same two sections at the midspans of the beam members of two indeterminate closed frames, there is very little indication of the section with compression steel and transverse ties being more ductile than the other section. The explanation is that the load carrying capacity of the frame with lateral ties and compression steel was being controlled by other hinging regions in the frame. Therefore, the curves for the sections in the indeterminate frame are not accurate indications of the difference in ductility of the two cross sections. The finding merits attention, and using cross sectional load-deformation data from a determinate member as a representation for the behavior of the same cross section in an indeterminate structure should be looked upon with caution.

Most researchers have found that decreasing the steel percentage

increases the rotational capacity of the section. This cannot be concluded from the test results because sufficient rotation data from Frame No. 1 and No. 3 were not obtained for comparison with Frame No. 2. This was due to improper location of the strain points in Frame No. 1 (the strain points were not located at the hinging regions) and a premature failure in Frame No. 3.

Examining Figure 25 at the corner where the column steel was bent in and the 90° hook was made in the top steel in the beam, it is noted that wide tension cracks opened in the concrete at this point. The steel from the beam which was bent down into the columns did not lap the point where the steel was bent in the columns to fully develop the strength of the section. The ACI Code's provision in Section 805(b) states that where splices are used, the length of lap should be 24 bar diameters or not less than 12 inches. This provision was not met in Frame No. 2, and the result is clearly indicated in Figure 24.

In Frame No. 3, a combination shear and bond failure occurred at the support as shown in Figure 27. A possible explanation is that the positive reinforcement from the midspan was terminated at the face of the column. This was done to avoid the congestion of reinforcement in the corners that was experienced in Frames No. 1 and No. 2. The ACI Code, Section 908(f) states specifically that at least one fourth the positive moment reinforcement should extend along the same face of the beam into the support at least six inches.

Thus, the provision of limit analysis to reduce the congestion

of reinforcement over the supports should be looked upon with caution. The ACI Code provisions in this area are good design guides for detailing the placement of reinforcing steel.

It should be noted that all frames were designed according to the assumption that no sidesway would occur. The desired collapse sequence was for the midspans to yield initially and rotate sufficiently for the moments to redistribute and form hinges in the corners, with no sidesway occurring. Frame No. 2 came the closest to forming this collapse mechanism. Frame No. 1 and Frame No. 3 sideswayed. Thus, it seems that the testing equipment should have included a restraining force against sidesway or otherwise the structure and the loading system would have to be perfectly symmetrical.

Also, having to predict where the hinges would form and where to locate the instrumentation proved difficult and limited the experimental data in some cases.

V. CONCLUSIONS

1. The maximum concrete compressive strain in a structural member at a section of maximum moment can be very much larger than the value of 0.003 in/in. given by the ACI Code 318-63.
2. The stress-strain curve for concrete, determined from a standard compression test, is not an accurate representation of the behavior of the same concrete in a structural member under a different state of stress.
3. Lateral ties and compression reinforcement increase the ductility of reinforced concrete members. Figure 29
4. Using cross section load-deformation data from a determinate member as a representation for the behavior of the same cross-section in an indeterminate structure should be looked upon with caution. Figure 29
5. The reduction of congestion of reinforcement provided by limit analysis should be looked upon cautiously. The ACI Code (Chapter 8 and 9) is a good design guide for the detailing of steel placement in reinforced concrete structures.
6. Limit Analysis comes closer to predicting the behavior of reinforced concrete structures than elastic analysis, but is still conservative in determining load carrying capacity. Table 3

LITERATURE CITED

1. Baker, A. L. L., "A Plastic Theory of Design for Ordinary Reinforced and Prestressed Concrete Including Moment Re-Distribution in Continuous Members," Magazine of Concrete Research, No. 2, June, 1949, Pages 57-66.

2. Chan, W. W. L., "The Ultimate Strength and Deformation of Plastic Hinges in Reinforced Concrete Frameworks," Magazine of Concrete Research, Volume 7, No. 21, November, 1955, Pages 121-132.

3. Chan, W. W. L., "The Rotation of Reinforced Concrete Plastic Hinges at Ultimate Load," Magazine of Concrete Research, Volume 14, No. 41, July, 1962, Pages 63-71.

4. Sawyer, H. A., Jr., "Status and Potentialities of Nonlinear Design of Concrete Frames," Flexural Mechanics of Reinforced Concrete - Proceedings of the International Symposium, Miami, Florida, November 10-12, 1964, Pages 7-28.

5. Sawyer, H. A., Jr., "Design of Concrete Frames for Two Failure Stages," Flexural Mechanics of Reinforced Concrete - Proceedings of the International Symposium, Miami, Florida, November 10-12, 1964, Pages 405-439.

6. Berwanger, Carl, "Limit Design by Successive Moment-Distribution," Journal of the Structural Division - Proceedings of the American Society of Civil Engineers, Volume 92, Number ST 1, February 1966, Pages 405-430.

7. Rosenblueth, Emilio; Díaz de Cossío, Roger, "Instability Consideration in Limit Design of Concrete Frames," Flexural Mechanics of

Reinforced Concrete - Proceedings of the International Symposium, Miami, Florida, November 10-12, 1964, Pages 439-463.

8. Roy, H. E. H.; Sozen, Mete A., "Ductility of Concrete," Flexural Mechanics of Reinforced Concrete - Proceedings of the International Symposium, Miami, Florida, November 10-12, 1964, Pages 213-224.

9. Bertero, Vitelmo V.; Felippa, C., Discussion of "Ductility of Concrete" by Roy, H. E. H.; Sozen, Mete A., Flexural Mechanics of Reinforced Concrete - Proceedings of the International Symposium, Miami, Florida, November 10-12, 1964, Pages 227-234.

10. Mattock, A. H., "Rotational Capacity of Hinging Regions in Reinforced Concrete Beams," Flexural Mechanics of Reinforced Concrete - Proceedings of the International Symposium, Miami, Florida, November 10-12, 1964, Pages 143-182.

11. Pfrang, E. O.; Siess, C. P.; Sozen, M. A., "Load-Moment-Curvature Characteristics of Reinforced Concrete Cross Sections," Journal of the American Concrete Institute, July, 1964, Volume 61, No. 7, Pages 763-778.

BIBLIOGRAPHY

1. Baker, A. L. L., "A Plastic Theory of Design for Ordinary Reinforced and Prestressed Concrete Including Moment Re-Distribution in Continuous Members," Magazine of Concrete Research, No. 2, June, 1949, Pages 57-66.

2. Barnard, Peter R., "The Collapse of Reinforced Concrete Beams," Flexural Mechanics of Reinforced Concrete - Proceedings of the International Symposium, Miami, Florida, November 10-12, 1964, Pages 501-520.

3. Bertero, Vitelmo V.; Felippa, C., Discussion of "Ductility of Concrete" by Roy, H. E. H.; Sozen, Mete A., Flexural Mechanics of Reinforced Concrete - Proceedings of the International Symposium, Miami, Florida, November 10-12, 1964, Pages 227-234.

4. Berwanger, Carl, "Limit Design by Successive Moment-Distribution," Journal of the Structural Division - Proceedings of the American Society of Civil Engineers, Volume 92, Number ST 1, February 1966, Pages 405-430.

5. Broms, Bengt B., "Stress Distribution, Crack Patterns, and Failure Mechanisms of Reinforced Concrete Members," Journal of the American Concrete Institute, Volume 61, December, 1964, Page 1535.

6. Burnett, E., "Flexural Rigidity, Curvature and Rotation and Their Significance in Reinforced Concrete Design," Magazine of Concrete Research, Volume 16, No. 47, June, 1964, Pages 67-72.

7. Chan, W. W. L., "The Rotation of Reinforced Concrete Plastic Hinges at Ultimate Load," Magazine of Concrete Research, Volume

14, No. 41, July, 1962, Pages 63-71.

8. Chan, W. W. L., "The Ultimate Strength and Deformation of Plastic Hinges in Reinforced Concrete Frameworks," Magazine of Concrete Research, Volume 7, No. 21, November, 1955, Pages 121-132.

9. Ernst, G. C., "Plastic Hinging at the Intersection of Beams and Columns," American Concrete Institute Journal, Volume 28, No. 12, June, 1957, Pages 1119-1144.

10. Ferguson, Phil M., "Long Reinforced Concrete Columns in Frames - Research at the University of Texas," Comité Européen Du Beton Flambement, October, 1966, Reprint from Preliminary Document, The University of Texas, Austin, Texas.

11. Mattock, A. H., "Rotational Capacity of Hinging Regions in Reinforced Concrete Beams," Flexural Mechanics of Reinforced Concrete - Proceedings of the International Symposium, Miami, Florida, November 10-12, 1964, Pages 143-182.

12. Murray, Kenneth Harold, "Experimental Studies on the Limit Analysis of Reinforced Concrete Fixed-Ended T-Beams," Thesis submitted to the Graduate Faculty of the Virginia Polytechnic Institute in candidacy for the degree of Master of Science in Structural Engineering, October, 1966, Blacksburg, Virginia.

13. Nordell, William J., "Hinging in Statically and Dynamically Loaded Reinforced Concrete Beams," October 1966, Naval Facilities Engineering Command, U. S. Naval Civil Engineering Laboratory, Technical Report R489, October, 1966.

14. Pfrang, E. O.; Siess, C. P.; Sozen, M. A., "Load-Moment-Curvature

Characteristics of Reinforced Concrete Cross Sections," Journal of the American Concrete Institute, July, 1964, Volume 61, No. 7, Pages 763-778.

15. Rosenblueth, Emilio; Díaz de Cossío, Roger, "Instability Consideration in Limit Design of Concrete Frames," Flexural Mechanics of Reinforced Concrete - Proceedings of the International Symposium, Miami, Florida, November 10-12, 1964, Pages 439-463.

16. Roy, H. E. H.; Sozen, Mete A., "Ductility of Concrete," Flexural Mechanics of Reinforced Concrete - Proceedings of the International Symposium, Miami, Florida, November 10-12, 1964, Pages 213-224.

17. Sawyer, H. A., Jr., "Design of Concrete Frames for Two Failure Stages," Flexural Mechanics of Reinforced Concrete - Proceedings of the International Symposium, Miami, Florida, November 10-12, 1964, Pages 405-439.

18. Sawyer, H. A., Jr., "Status and Potentialities of Nonlinear Design of Concrete Frames," Flexural Mechanics of Reinforced Concrete - Proceedings of the International Symposium, Miami, Florida, November 10-12, 1964, Pages 7-28.

19. Winter, George; Urquhart, L. C.; O'Rourke, C. E.; Nilson, Arthur H., Design of Concrete Structures, McGraw-Hill Book Company, New York, San Francisco, Toronto, London, Copyright 1958, 1964, Chapters 3 and 5.

20. Wright, D. T.; Berwanger, C., "Limit Design of Reinforced Concrete Beams," Journal of the Structural Division - Proceedings of the American Society of Civil Engineers, Volume 86, Number ST 7, July, 1960, Pages 1-37.

The vita has been removed from the scanned document

APPENDIX A

TABLE 4.

LOAD-ROTATION DATA FOR FRAME NO.1

AT

CENTERLINE OF BEAM

LOAD (KIPS)	ROTATION (RADIANS)	DEPTH TO N.A. (INCHES)	STRAIN (EC) (IN./IN.)
0.49	0.00000	0.00	0.00000
1.13	0.60120	5.99	0.00018
1.77	1.20240	3.50	0.00021
2.30	2.60521	1.38	0.00018
2.73	3.60721	1.83	0.00033
3.16	4.40882	2.13	0.00047
3.48	4.40882	1.91	0.00042
3.69	4.40882	2.81	0.00062
3.90	5.21042	2.73	0.00071
4.01	5.01002	2.80	0.00070
4.09	7.01403	2.28	0.00080
4.14	8.21643	2.22	0.00091
4.22	9.81964	2.32	0.00114
4.33	12.02405	2.25	0.00135
4.44	14.42886	2.11	0.00152
4.60	17.63527	1.91	0.00168
4.60	24.24850	1.82	0.00221
3.90	37.87575	1.82	0.00344
3.96	42.68537	1.84	0.00393
3.90	50.90180	1.90	0.00485
3.80	60.32064	1.99	0.00602
3.58	69.33868	2.04	0.00707
3.28	78.35671	2.26	0.00887

NOTE- ROTATION VALUES HAVE BEEN MULTIPLIED BY 10**3

TABLE 5.

LOAD-ROTATION DATA FOR FRAME NO.1

AT

CENTERLINE OF COLUMN

LOAD (KIPS)	ROTATION (RADIANS)	DEPTH TO N.A. (INCHES)	STRAIN (EC) (IN./IN.)
0.49	0.00000	0.00	0.00000
1.13	0.05263	2.55	0.00000
1.77	0.15789	3.18	0.00003
2.30	0.28421	3.68	0.00005
2.73	0.34737	3.93	0.00007
3.16	0.44211	3.95	0.00009
3.48	0.50526	3.89	0.00010
3.69	0.53684	3.78	0.00010
3.90	0.58947	3.84	0.00011
4.01	0.63158	3.82	0.00012
4.09	0.67368	3.80	0.00013
4.14	0.71579	3.78	0.00014
4.22	0.75789	3.76	0.00014
4.33	0.80000	3.75	0.00015
4.44	0.92632	3.50	0.00018
4.60	1.02105	3.75	0.00015
4.60	1.15789	3.50	0.00020
3.90	1.07368	3.41	0.00018
3.96	1.07368	3.41	0.00018
3.90	1.05263	3.31	0.00017
3.80	1.03158	3.31	0.00017
3.58	1.01053	3.31	0.00017
3.28	1.03158	3.31	0.00017

NOTE- ROTATION VALUES HAVE BEEN MULTIPLIED
BY 10**3

TABLE 6.

LOAD-ROTATION DATA FOR FRAME NO.2

AT

CENTERLINE OF BEAM

LOAD (KIPS)	ROTATION (RADIANS)	DEPTH TO N.A. (INCHES)	STRAIN (EC) (IN./IN.)
0.17	0.00000	0.00	0.00000
0.72	0.20040	5.99	0.00006
1.45	-0.20040	-3.99	0.00004
2.25	1.00200	3.99	0.00020
2.89	1.80361	2.66	0.00024
3.42	2.60521	2.92	0.00038
3.69	2.80561	2.43	0.00034
3.90	3.60721	2.11	0.00038
4.12	3.00601	1.67	0.00025
4.33	4.00802	3.00	0.00060
4.28	6.01202	2.00	0.00060
4.12	16.03206	1.50	0.00120
3.96	30.26052	1.20	0.00181
3.80	41.48297	1.36	0.00282
3.70	48.69739	1.31	0.00318
3.69	57.51503	1.45	0.00418
3.64	61.32264	1.44	0.00442
3.59	67.33467	1.39	0.00467
3.64	71.94389	1.35	0.00485
3.49	76.95391	1.43	0.00550
3.53	77.15431	1.44	0.00556

NOTE- ROTATION VALUES HAVE BEEN MULTIPLIED BY 10**3

TABLE 7.

LOAD-ROTATION DATA FOR FRAME NO.2

AT

CENTERLINE OF COLUMN

LOAD (KIPS)	ROTATION (RADIANS)	DEPTH TO N.A. (INCHES)	STRAIN (EC) (IN./IN.)
0.17	0.00000	0.00	0.00000
0.72	0.97561	2.92	0.00014
1.45	1.75610	3.15	0.00028
2.25	1.56098	3.44	0.00027
2.89	2.92683	2.58	0.00038
3.42	2.34146	2.58	0.00030
3.69	2.92683	2.58	0.00038
3.90	2.92683	1.90	0.00028
4.12	2.73171	2.71	0.00037
4.33	2.14634	3.20	0.00034
4.28	3.90244	2.67	0.00052
4.12	2.73171	2.71	0.00037
3.96	2.73171	2.71	0.00037
3.80	2.92683	2.58	0.00038
3.70	1.95122	3.44	0.00034
3.69	1.56098	3.44	0.00027
3.64	1.75610	3.15	0.00028
3.59	1.95122	3.95	0.00039
3.64	2.73171	3.44	0.00047
3.49	2.53659	3.24	0.00041
3.53	2.53659	3.24	0.00041

NOTE- ROTATION VALUES HAVE BEEN MULTIPLIED BY 10**3

TABLE 8.

LOAD-ROTATION DATA FOR FRAME NO.2

AT

LEFT

LOAD (KIPS)	ROTATION (RADIANS)	DEPTH TO N.A. (INCHES)	STRAIN (EC) (IN./IN.)
0.17	0.00000	0.00	0.00000
0.72	-0.44444	8.13	-0.00018
1.45	-0.44444	5.88	-0.00013
2.25	0.22222	-7.63	-0.00008
2.89	1.11111	2.27	0.00013
3.42	1.11111	0.48	0.00003
3.69	2.22222	2.72	0.00030
3.90	2.22222	1.38	0.00011
4.12	2.44444	1.78	0.00022
4.33	2.66667	1.75	0.00023
4.28	4.00000	1.62	0.00033
4.12	11.11111	1.73	0.00096
3.96	20.66667	1.38	0.00145
3.80	31.55556	1.76	0.00277
3.70	40.22222	1.65	0.00332
3.69	48.44444	1.62	0.00393
3.64	57.33333	1.60	0.00459
3.59	68.00000	1.70	0.00577
3.64	77.33333	1.71	0.00662
3.49	87.11111	1.75	0.00764
3.53	87.11111	1.75	0.00764

NOTE- ROTATION VALUES HAVE BEEN MULTIPLIED BY 10**3

TABLE 9.

LOAD-ROTATION DATA FOR FRAME NO.2

AT

RIGHT

LOAD (KIPS)	ROTATION (RADIANS)	DEPTH TO N.A. (INCHES)	STRAIN (EC) (IN./IN.)
0.17	0.00000	0.00	0.00000
0.72	0.00000	0.00	0.00000
1.45	-0.40000	6.00	-0.00012
2.25	1.40000	3.86	0.00027
2.89	1.00000	2.00	0.00010
3.42	1.00000	4.00	0.00020
3.69	0.60000	-0.67	-0.00002
3.90	1.20000	1.00	0.00006
4.12	1.40000	1.71	0.00012
4.33	2.40000	1.83	0.00022
4.28	3.20000	1.63	0.00026
4.12	10.00000	1.30	0.00065
3.96	19.80000	0.90	0.00089
3.80	29.00000	1.00	0.00146
3.70	39.20000	1.00	0.00196
3.69	48.00000	1.00	0.00240
3.64	56.40000	1.00	0.00282
3.59	63.00000	0.98	0.00310
3.64	70.20000	1.03	0.00361
3.49	70.20000	1.03	0.00361
3.53	70.20000	1.03	0.00361

NOTE- ROTATION VALUES HAVE BEEN MULTIPLIED BY 10**3

TABLE 10.

LOAD-ROTATION DATA FOR FRAME NO.3

AT

CENTERLINE OF BEAM

LOAD (KIPS)	ROTATION (RADIANS)	DEPTH TO N.A. (INCHES)	STRAIN (EC) (IN./IN.)
0.22	0.00000	0.00	0.00000
0.78	-0.40282	5.96	-0.00012
1.28	0.40282	5.96	0.00012
1.72	1.40987	6.67	0.00047
2.20	2.21551	5.96	0.00066
2.46	3.42397	4.80	0.00082
2.84	4.63243	4.45	0.00103
3.05	4.22961	3.60	0.00076
3.21	4.43102	3.71	0.00082
3.37	5.43807	3.39	0.00092
3.60	5.84089	2.71	0.00079
3.74	7.25076	2.93	0.00106
2.84	16.51561	1.85	0.00153

NOTE- ROTATION VALUES HAVE BEEN MULTIPLIED BY 10**3

TABLE 11.

LOAD-ROTATION DATA FOR FRAME NO.3

AT

CENTERLINE OF COLUMN

LOAD (KIPS)	ROTATION (RADIANS)	DEPTH TO N.A. (INCHES)	STRAIN (EC) (IN./IN.)
0.22	0.00000	0.00	0.00000
0.78	-0.00000	0.00	0.00000
1.28	-0.40000	13.31	-0.00027
1.72	1.80000	4.70	0.00042
2.20	2.40000	2.89	0.00035
2.46	1.80000	4.70	0.00042
2.84	1.80000	3.03	0.00027
3.05	2.80000	4.38	0.00061
3.21	2.80000	2.60	0.00036
3.37	3.20000	3.00	0.00048
3.60	3.40000	2.57	0.00044
3.74	3.00000	2.48	0.00037
2.84	2.60000	3.12	0.00041

NOTE- ROTATION VALUES HAVE BEEN MULTIPLIED BY 10**3

TABLE 12.

LOAD-ROTATION DATA FOR FRAME NO.3

AT

LEFT

LOAD (KIPS)	ROTATION (RADIANS)	DEPTH TO N.A. (INCHES)	STRAIN (EC) (IN./IN.)
0.22	0.00000	0.00	0.00000
0.78	0.18389	0.88	-0.00000
1.28	-0.73556	7.67	-0.00028
1.72	-0.18389	-10.00	0.00009
2.20	-0.36778	6.31	-0.00012
2.46	1.10335	2.69	0.00015
2.84	0.91946	0.88	0.00005
3.05	1.28724	2.43	0.00016
3.21	1.65502	2.08	0.00017
3.37	1.65502	1.48	0.00012
3.60	2.94226	1.90	0.00028
3.74	3.49393	1.45	0.00025
2.84	20.22802	0.93	0.00094

NOTE- ROTATION VALUES HAVE BEEN MULTIPLIED BY 10**3

TABLE 13.

LOAD-ROTATION DATA FOR FRAME NO.3

AT

RIGHT

LOAD (KIPS)	ROTATION (RADIANS)	DEPTH TO N.A. (INCHES)	STRAIN (EC) (IN./IN.)
0.22	0.00000	0.00	0.00000
0.78	0.39506	5.94	0.00012
1.28	1.38272	4.49	0.00031
1.72	0.59259	2.56	0.00008
2.20	0.59259	9.31	0.00028
2.46	0.19753	16.06	0.00016
2.84	0.39506	13.53	0.00027
3.05	0.98765	5.94	0.00029
3.21	1.58025	4.67	0.00037
3.37	1.38272	5.22	0.00036
3.60	1.97531	2.39	0.00024
3.74	2.37037	2.14	0.00025
2.84	29.43210	0.98	0.00144

NOTE- ROTATION VALUES HAVE BEEN MULTIPLIED
BY 10**3

APPENDIX B

TABLE 14

LOAD DEFLECTION DATA FOR FRAME NO. 1

Load (Kips)	Deflection Of Beam (Inches)	Deflection Of Column (Inches)	Corner Rotation (Radians x 10^3)
0.49	0.000	0.000	0.000
1.13	0.020	0.004	1.125
1.77	0.052	0.018	6.500
2.30	0.092	0.042	8.350
2.73	0.118	0.058	11.000
3.16	0.150	0.075	19.800
3.48	0.174	0.089	21.500
3.69	0.190	0.098	22.500
3.90	0.208	0.106	26.600
4.01	0.230	0.114	26.600
4.09	0.255	0.125	27.200
4.14	0.277	0.135	27.200
4.22	0.299	0.146	30.600
4.33	0.324	0.158	32.500
4.44	0.377	0.179	36.400
4.60	0.451	0.206	39.200
4.60	0.556	0.226	17.600
3.90	0.832	0.196	15.300
3.96	0.930	0.274	15.900
3.90	1.042	0.318	17.400
3.80	1.242	0.344	18.000
3.58	1.430	0.372	22.800
3.28	1.635	0.393	-

TABLE 15

LOAD DEFLECTION DATA FOR FRAME NO. 2

Load (Kips)	Deflection Of Beam (Inches)	Deflection Of Column (Inches)	Corner Rotation (Radians x 10^4)
0.17	0.000	0.000	0.000
0.72	0.015	0.007	6.750
1.45	0.030	0.014	13.500
2.25	0.072	0.036	35.500
2.89	0.110	0.059	60.750
3.42	0.136	0.072	79.000
3.69	0.154	0.080	90.250
3.90	0.166	0.085	97.750
4.12	0.182	0.092	114.000
4.33	0.194	0.097	123.750
4.28	0.240	0.102	157.250
4.12	0.418	0.121	280.500
3.96	0.678	0.150	504.750
3.80	0.892	0.174	631.500
3.70	1.131	0.199	793.500
3.69	1.354	0.219	954.500
3.64	1.582	0.237	1112.750
3.59	1.795	0.252	1252.750
3.64	2.013	0.271	1439.500
3.49	2.238	0.292	-
3.53	2.409	0.313	-

TABLE 16

LOAD DEFLECTION DATA FOR FRAME NO. 3

Load (Kips)	Deflection Of Beam (Inches)	Deflection Of Column (Inches)	Corner Rotation (Radians x 10^3)
0.22	0.000	0.000	0.000
0.78	0.011	0.005	0.006
1.28	0.032	0.014	0.001
1.72	0.065	0.032	0.005
2.20	0.101	0.053	0.009
2.46	0.126	0.068	0.011
2.84	0.159	0.086	0.013
3.05	0.179	0.097	0.014
3.21	0.197	0.107	0.015
3.37	0.221	0.187	0.016
3.61	0.244	0.192	0.017
3.74	0.266	0.205	0.019
2.84	0.445	0.215	-

APPENDIX C

FORTRAN PROGRAM

```
$IBJOB
$IBFTC          NODECK
C     PSI(1,I)= PRESSURE ON EACH OF THREE
C                HYDRAULIC LOADING JACKS
C     P(I)= LOAD (KIPS)
C     I= NUMBER OF READING
C     M= TOTAL NUMBER OF READINGS
C     DEPTH(J)= VERTICAL DISTANCE BETWEEN STRAIN
C                POINTS (INCHES)
C     DISTST(J)= DISTANCE FROM EXTREME COMPRESSION
C                 FIBER TO STRAIN GAGE IN COMPRESSIVE
C                 REGION
C     S(J,I)= STRAIN GAGE READING (J= NO. OF POSITION
C              OF STRAIN GAGE )
C     SI(J)= INITIAL STRAIN GAGE READING AT APPLIED
C             INITIAL LOAD
C     ROTCLB= ROTATION AT CENTER OF BEAM (RADIANS)
C     ROTCLC= ROTATION AT CENTER OF COLUMN (RADIANS )
C     ROTLT= ROTATION OF LEFT CORNER SECTION (RADIANS)
C     ROTRT= ROTATION OF RIGHT CORNER SECTION (RADIANS)
C     J=1 AT CENTER SECTION OF BEAM
C     J=2 AT CENTER SECTION OF COLUMN
```

```
C     J=3 AT LEFT CORNER SECTION
C     J=4 AT RIGHT CORNER SECTION
C     CONST(J,I)= CONCRETE STRAIN(EC) AT EXTREME
C                 COMPRESSION FIBER
C     DEFCLB(I)= CENTERLINE DEFLECTION OF BEAM
C                (INCHES)
C     TOPST(J,I)= STRAIN AT GAGE IN COMPRESSION
C                 REGION
C     BOTST(J,I)= STRAIN AT GAGE IN TENSION
C                 REGION
C     DNA(J,I)= DEPTH FROM EXTREME COMPRESSION FIBER
C               TO NEUTRAL AXIS (INCHES)
      DIMENSION S(8,30),SI(8),PSI(30),P(30),ROTCLB(30),
     1 ROTCLC(30),ROTLT(30),ROTRT(30),DNA(8,30),BOTST(8,30),
     2 TOPST(8,30),CONST(8,30),DEPTH(8),DISTST(8)
      M=21
      READ(5,1) (DEPTH(J),J=1,4)
    1 FORMAT (4F6.4)
      READ (5,2) (DISTST(J),J=1,4)
    2 FORMAT (4F6.4)
      READ(5,3) SI
      READ(5,3) ((S(J,I),J=1,8),I=2,M)
    3 FORMAT (8F5.1)
```

```
      READ(5,4) (PSI(I),I=1,M)
    4 FORMAT(10F5.1/10F5.1/1F5.1)
      ROTCLB(1)=0.0
      ROTCLC(1)=0.0
      ROTLT(1)=0.0
      ROTRT(1)=0.0
      WRITE(7,5)
    5 FORMAT(17X,33HLOAD-ROTATION DATA FOR FRAME NO.2//
     1 32X,2HAT/)
      DO 6 I=1,M
    6 P(I)=(10.867*PSI(I)+62.724)*0.001
      DO 13 I=2,M
      TOPST(1,I)= S(1,I)-SI(1)
      BOTST(1,I)= SI(2)-S(2,I)
      TOPST(2,I)= S(3,I)-SI(3)
      BOTST(2,I)= SI(4)-S(4,I)
      TOPST(3,I)= S(5,I)-SI(5)
      BOTST(3,I)=SI(6)-S(6,I)
      TOPST(4,I)= S(7,I)-SI(7)
      BOTST(4,I)= SI(8)-S(8,I)
      ROTCLB(I)=(TOPST(1,I)+BOTST(1,I))/DEPTH(1)
      ROTCLC(I)=(TOPST(2,I)+BOTST(2,I))/DEPTH(2)
      ROTLT(I)=(TOPST(3,I)+BOTST(3,I))/DEPTH(3)
```

```
      ROTRT(I)=(TOPST(4,I)+BOTST(4,I))/DEPTH(4)
      DO 7 J=1,4
      IF (TOPST(J,I)+BOTST(J,I)) 8,9,8
    8 DNA(J,I)= (TOPST(J,I)*DEPTH(J)/(TOPST(J,I)+
     1BOTST(J,I)))+DISTST(J)
      GO TO 7
    9 DNA(J,I)=0.000
    7 CONST(J,I)=0.000
      DO 13 J=1,4
      IF (DNA(J,I)) 11,12,11
   11 CONST(J,I)=(TOPST(J,I)*DNA(J,I)/(DNA(J,I)-
     1DISTST(J)))*0.00005
      GO TO 13
   12 CONST(J,I)=0.000
   13 CONTINUE
      WRITE(7,20)
   20 FORMAT(23X,18HCENTERLINE OF BEAM//13X,4HLOAD,3X,
     1 18HROTATION,3X,13HDEPTH TO N.A.,3X,11HSTRAIN (EC)/
     2 12X,6H(KIPS),2X,9H(RADIANS),4X,8H(INCHES),
     3 7X,9H(IN./IN.))
      DO 21 I=1,M
   21 WRITE(7,22) P(I),ROTCLB(I), DNA(1,I), CONST(1,I)
   22 FORMAT (11X,F6.2,2X,F9.5,5X,F6.2,9X,F8.5)
```

```
      WRITE(7,5)
      WRITE(7,23)
   23 FORMAT(22X,20HCENTERLINE OF COLUMN//13X,4HLOAD,3X,
     18HROTATION,3X,13HDEPTH TO N.A.,3X,11HSTRAIN (EC)/
     212X,6H(KIPS),2X,9H(RADIANS),4X,8H(INCHES),
     37X,9H(IN./IN.))
      DO 24 I=1,M
   24 WRITE(7,25)P(I), ROTCLC(I), DNA(2,I), CONST(2,I)
   25 FORMAT (11X,F6.2,2X,F9.5,5X,F6.2,9X,F8.5)
       WRITE(7,5)
      WRITE(7,26)
   26 FORMAT(31X,4HLEFT//13X,4HLOAD,3X,
     18HROTATION,3X,13HDEPTH TO N.A.,3X,11HSTRAIN (EC)/
     212X,6H(KIPS),2X,9H(RADIANS),4X,8H(INCHES),
     37X,9H(IN./IN.))
      DO 27 I=1,M
   27 WRITE(7,28) P(I), ROTLT(I), DNA(3,I), CONST(3,I)
   28 FORMAT (11X,F6.2,2X,F9.5,5X,F6.2,9X,F8.5)
       WRITE(7,5)
      WRITE(7,29)
   29 FORMAT(31X,5HRIGHT//13X,4HLOAD,3X,
     18HROTATION,3X,13HDEPTH TO N.A.,3X,11HSTRAIN (EC)/
     212X,6H(KIPS),2X,9H(RADIANS),4X,8H(INCHES),
```

```
     37X,9H(IN./IN.))
      DO 30 I=1,M
   30 WRITE (7,31) P(I), ROTRT(I), DNA(4,I), CONST(4,I)
   31 FORMAT (11X,F6.2,2X,F9.5,5X,F6.2,9X,F8.5)
   50 STOP
      END
$ENTRY
DATA DECK
$IBSYS
```

ANALYTICAL AND EXPERIMENTAL STUDIES ON REINFORCED CONCRETE CLOSED FRAMES

by

Charles W. Pryor, Jr.

Abstract

Researchers have recently found that reinforced concrete can display enough plastic stability to enhance the development of a limit analysis for concrete similar to plastic analysis for structural steel. The development of limit analysis depends upon a favorable comparison of experimental test results with analytical predictions. The purpose of this investigation is to compare experimental test results with analytical predictions, using both a conventional elastic analysis and a limit analysis, for reinforced concrete closed frames.

The test frames were rectangular, six feet in width by five feet in height, and were loaded by three hydraulic jacks. All members were four inches wide by seven inches deep. The parameters investigated were the reinforcing steel percentage, the contribution of lateral ties and compression steel to the rotational capacity and the effect of steel placement and concrete cover on the load carrying capacity.

The methods used in analyzing the frames were elastic analysis using the ACI Code 318-63, limit analysis using moment-area concepts and a bilinear approximation to the moment-curvature curve, and limit analysis using successive moment distribution and an elasto-

plastic approximation to the moment-curvature curve.

Test results are presented in the form of load-rotation curves and tables showing maximum concrete strains and neutral axis depths. A comparison of predicted ultimate loads with experimental ultimate loads is presented in tabulated form.

From the investigation, it was concluded that limit analysis more accurately predicts the load carrying capacity of reinforced concrete frames, but is still a conservative method of analysis.